Hindawi
Complexity
Volume 2022, Article ID 4112362, 25 pages
https://doi.org/10.1155/2022/4112362

Research Article

On Topological Analysis of Niobium (II) Oxide Network via Curve Fitting and Entropy Measures

Muhammad Kamran Siddiqui,[1] Sana Javed,[1] Sadia Khalid,[1] Mazhar Hussain,[1] Muhammad Shahbaz,[1] and Samuel Asefa Fufa[2]

[1]*Department of Mathematics, COMSATS University Islamabad, Lahore Campus, Pakistan*
[2]*Department of Mathematics, Addis Ababa University, Addis Ababa, Ethiopia*

Correspondence should be addressed to Samuel Asefa Fufa; samuel.asefa@aau.edu.et

Received 24 April 2022; Revised 26 May 2022; Accepted 21 June 2022; Published 13 August 2022

Academic Editor: Yue Song

The remarkable optical features of metallic nanoparticles have extensively developed the interest of scientists and researchers. The generated heat overwhelms cancer tissue incident to nanoparticles with no damage to sound tissues. Niobium nanoparticles have the ability of easy ligands connection so they are very suitable in treating cancer optothermally. A modern field of applied chemistry is chemical graph theory. With the use of combinatorial methods, such as vertex and edge partitions, we explore the connection between atoms and bonds. Topological indices play a vital part in equipping directions to treat cancers or tumors. These indices might be derived experimentally or computed numerically. Although experimental results are worthful but they are expensive as well, so computational analysis provides an economical and rapid way. A topological index is a numerical value that is only determined by the graph. In this paper, we will discuss the chemical graph of niobium (II) oxide. Additionally, each topological index is related with thermodynamical properties of niobium (II) oxide, including entropy and enthalpy. This has been done in MATLAB software, using rational built-in method.

1. Introduction

All types of data quantitative, qualitative, processed, or unprocessed might be considered to gain information to address a simple or a complicated event or situation. If we consider the flow chart of the information, then on the top of the hierarchy we would find notion being the first qualitative obscure assessment of information. The central part of this flow chart comprises of the parameters and measurements while decision making extracted from inference is the final step. Different properties of a chemical compound like its nature, atoms, or chemical state provide us chemical information about the structure [1]. Different chemical reactions in a substance environment produce different physicochemical properties/activities that include boiling point, entropy, heat of formation, or density. In this way, the whole milieu of a substance becomes a promising root of information for the analysis of its chemistry [1]. Supplementary knowledge might be gained by *in silico* trials for the designing of new compounds for a specified study or objective. Stimulation in such approaches has been seen due to expensive experimental studies along with rigorous biotic and ecological regulations [2]. Such *in silico* studies are very progressive in medicine due to their cost effectiveness.

Different approaches including graphical quantitative/quantitative structure activity/property relationship (QSAR/QSPR) and modeling have become an essential part of *in silico* studies in drug development [3, 4]. This is due to the fact that biological variations can be explained in the form of chemical variations. Such analyses are performed continually to obtain profound results [5, 6]. Topological indices play a vital part in equipping directions to treat cancers or tumors. These indices might be derived experimentally or computed numerically [7, 8]. Although experimental results are worthful but they are expensive as well, so computational analysis provides an economical way Recently, several studies are performed/reviewed using the concept of graph theoretical indices in drug research [9, 10]. There is a wide variety of such indices in the literature [11, 12].

A graph usually comprises of two sets, namely, vertex set, that contains the objects, and the edge set; this is based on the connections between the objects. Any chemical compound might be represented in the form of a graph where atoms make the vertex set and the bonding between atoms creates the edge set. Topological indices are based on the atomic connectivity table of the chemical compound [1]. Graphical descriptors, which are usually defined in the form of numerical numbers, can be used to appraise distinct immersed characteristics of a chemical compound from different point of view. Zagreb indices measure the compactness of a molecule so it can be correlated with the physicochemical properties of a compound which depend on the volume/surface ratio of the molecules.

The remarkable optical features of metallic nanoparticles have extensively developed the interest of scientists and researchers [13–15]. Researchers have analyzed that the thermoplasmonic features of nanoparticles might be utilized in treating cancers [16–18]. In optothermal cancer tissue therapy, the descendent laser light provokes the frequency of maximum response amplitude of external plasmon of metallic nanoparticles and consequently the immersed energy of descendent light preserves the heat in nanoparticles [19–21]. The generated heat overwhelms cancer tissue incident to nanoparticles with no damage to sound tissues [22, 23]. Niobium nanoparticles have the ability of easy ligands connection so they are very suitable in treating the cancer optothermally [24–26].

Niobium (Nb), a recalcitrant metal, is a suitable construction material for the first shell of nuclear fusion reactors [27]. It does, however, have a high affinity for oxygen and carbon, which are found in pyrotechnics and refrigerants such as liquid. Niobium is renowned to interact very efficiently with oxygen as a component for the first barrier. As a result, reliable thermodynamical data on niobium oxides, NbO, NbO_2, Nb_2O_5, and other intermediary phases, such as $Nb_{12}O_{29}$, are useful. Apart from that, niobium oxides have a variety of innovative uses. Niobium monoxide (NbO) is utilized as a gate electrode in transistors [28], and a (NbO/NbO_2) junction may be employed in robust switching devices [29]. NbO crystallises in the form of a face-centered cubic structure similar to sodium chloride crystal where every Nb atom in a square planar lattice is linked to four oxygen atoms [30]. Furthermore, the NbO crystal structure is unique in which it has 25 percent arranged voids in both the Nb and O sublattices as shown in Figure 1 [31].

Researchers have investigated the electrical and thermophysical properties of NbO. NbO has a density of around $7.3 g/cm^3$ and a melting temperature of 1940°C [31]. Niobium monoxide exhibits typical metallic behaviour and is usually recognised as a metal, with a resistivity of around $21 l \times$ cm at 25°C that drops with temperature to $1.8 l \times$ cm at 4.2 k. Researchers have measured X-ray fluorescence for several niobium oxides and correlated the findings of NbO to the conduction and valence band calculations of $Nb_{1.0}O_{\infty}$!, discovering substantial variances [32]. They attempted to emulate the NbO structure by doing band structure calculations for $Nb_{0.75}O_{0.75}$ in order to account for the 25% vacancy (see Figure 1). However, the investigation pertaining to the thermodynamic data is very scarce. The laboratory work to study these characteristics is limited due to the analytical limitations. Therefore, computational techniques can be applied to estimate their thermodynamic characteristics. Topological study is useful in this regard [31].

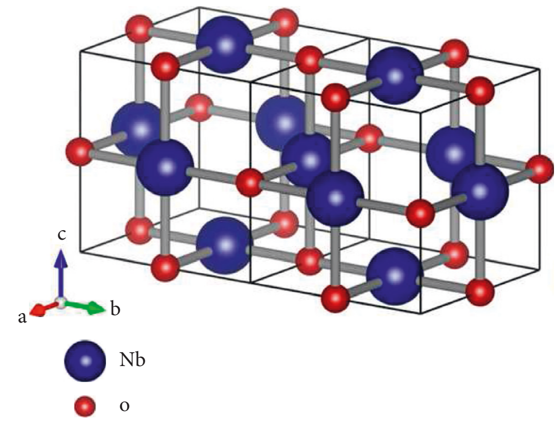

Figure 1: Cubic structure of NbO.

Milan Randić presented the following index, namely, General Randić index [33–35] for a graph $G = (V, E)$, where $\mathfrak{L}(a)$ denotes the degree of a vertex a as the number of edges with a:

$$R_\alpha(G) = R_\alpha = \sum_{lm \in E(G)} (\mathfrak{L}(l) \times \mathfrak{L}(m))^\alpha, \quad \text{where } \alpha \in \left\{1, -1, \frac{1}{2}, -\frac{1}{2}\right\}, 2. \tag{1}$$

Estrada et al. [36, 37] established atom bond connectivity index as follows:

$$\mathrm{ABC}(G) = \mathrm{ABC} = \sum_{lm \in E(G)} \sqrt{\frac{\mathfrak{L}(l) + \mathfrak{L}(m) - 2}{\mathfrak{L}(l) \times \mathfrak{L}(m)}}. \tag{2}$$

Vukičević and Furtula [38] presented the geometric arithmetic index as follows:

$$GA(G) = GA = \sum_{lm \in E(G)} \frac{2\sqrt{\mathfrak{L}(l) \times \mathfrak{L}(m)}}{\mathfrak{L}(l) + \mathfrak{L}(m)}. \tag{3}$$

The Zagreb indices defined in [20, 39, 40] are as follows:

$$M_1(G) = M_1 = \sum_{lm \in E(G)} (\mathfrak{L}(l) + \mathfrak{L}(m)), \quad M_2(G) = M_2 = \sum_{lm \in E(G)} (\mathfrak{L}(l) \times \mathfrak{L}(m)). \tag{4}$$

The first and second Zagreb coindices defined in [41, 42] are as follows:

$$\overline{M}_1(G) = \overline{M}_1 = \sum_{lm \notin E(G)} (\mathfrak{L}(l) + \mathfrak{L}(m)), \quad \overline{M}_2(G) = \overline{M}_2 = \sum_{lm \notin E(G)} (\mathfrak{L}(l) \times \mathfrak{L}(m)). \tag{5}$$

Gutman and Trinajstić [40] and Furtula and Gutman [43] introduced forgotten index as follows:

$$F(G) = F = \sum_{lm\in E(G)} \left(\mathfrak{L}(l)^2 + \mathfrak{L}(m)^2\right). \tag{6}$$

Wang et al. [44] described the augmented Zagreb index as

$$\mathrm{AZI}(G) = \mathrm{AZI} = \sum_{lm\in E(G)} \left(\frac{\mathfrak{L}(l)\times\mathfrak{L}(m)}{\mathfrak{L}(l)+\mathfrak{L}(m)-2}\right)^3. \tag{7}$$

The Balaban index [45, 46] is presented as follows:

$$J(G) = J = \frac{l}{l-m}\sum_{lm\in E(G)} \frac{1}{\mathfrak{L}(l)\times\mathfrak{L}(m)}. \tag{8}$$

Ranjini et al. in [47] reformulated versions of Zagreb indices as follows:

$$\begin{aligned}
\mathrm{ReZG}_1(G) &= \mathrm{ReZG}_1 = \sum_{lm\in E(G)} \frac{\mathfrak{L}(l)+\mathfrak{L}(m)}{\mathfrak{L}(l)\times\mathfrak{L}(m)},\\
\mathrm{ReZG}_2(G) &= \mathrm{ReZG}_2 = \sum_{lm\in E(G)} \frac{\mathfrak{L}(l)\times\mathfrak{L}(m)}{\mathfrak{L}(l)+\mathfrak{L}(m)},\\
\mathrm{ReZG}_3(G) &= \mathrm{ReZG}_3\\
&= \sum_{lm\in E(G)} (\mathfrak{L}(l)\times\mathfrak{L}(m))(\mathfrak{L}(l)+\mathfrak{L}(m)).
\end{aligned} \tag{9}$$

2. Results for Niobium (II) Oxide

The number of vertices and edges of structure of Niobium (II) oxide denoted by NbO is $9lm + 5l + 5m + 2$ and $16lm + 6l + 6m$, respectively. In NbOthere are three types of vertices, namely, the vertices of degree 2,3, and 4, respectively. The vertex and edge partition of NbO is presented in Table 1 and Table 2, respectively.

Table 1: Vertex partition of NbO.

$\mathfrak{L}(v)$	Frequency	Set of vertices
2	8	V_1
3	$4lm + 8l + 8m - 8$	V_3
4	$5lm - 3l - 3m + 2$	V_4

Table 2: Edge partition of NbO.

$(\mathfrak{L}(l), \mathfrak{L}(m))$	Frequency	Set of edges
(2, 3)	16	E_1
(3, 3)	$16l + 16m - 24$	E_2
(3, 4)	$12lm - 8l - 8m + 8$	E_3
(4, 4)	$4lm - 2l - 2m$	E_4

Theorem 1. *Let $G \cong NbO[l,m]$ with $l,m \geq 1$. Then, Randić indices for $\alpha \in \{1,-1,(1/2),-(1/2)\}$ are as follows:*

$$\begin{aligned}
R_1 &= 208lm + 16l + 16m - 24,\\
R_{-1} &= 1.125lm + 1.1111l + 0.9861m + 0.6666,\\
R_{1/2} &= 49.5692lm + 20.2871l + 12.2871m - 5.0953,\\
R_{-(1/2)} &= 3.9641lm + 3.0239l + 2.5239m + 0.8413.
\end{aligned} \tag{10}$$

Proof. For $\alpha = 1$,

$$\begin{aligned}
R_1 &= \sum_{lm\in E(G)} \mathfrak{L}(l)\times\mathfrak{L}(m)\\
&= (16)(6) + (16l + 16m - 24)(9)\\
&\quad + (12lm - 8l - 8m + 8)(12) + (4lm - 2l - 2m)(16)\\
&= 208lm + 16l + 16m - 24.
\end{aligned} \tag{11}$$

For $\alpha = -1$,

$$\begin{aligned}
R_{-1} &= \sum_{lm\in E(G)} \frac{1}{\mathfrak{L}(l)\times\mathfrak{L}(m)}\\
&= (16)\left(\frac{1}{6}\right) + (16l + 16m - 24)\left(\frac{1}{9}\right)\\
&\quad + (12lm - 8l - 8m + 8)\left(\frac{1}{12}\right)\\
&\quad + (4lm - 2l - 2m)\left(\frac{1}{16}\right)\\
&= 1.125lm + 1.1111l + 0.9861m + 0.6666.
\end{aligned} \tag{12}$$

For $\alpha = 1/2$,

$$\begin{aligned}
R_{1/2} &= \sum_{lm\in E(G)} \sqrt{\mathfrak{L}(l)\times\mathfrak{L}(m)}\\
&= (16)(\sqrt{6}) + (16l + 16m - 24)(\sqrt{9})\\
&\quad + (12lm - 8l - 8m + 8)(\sqrt{12})\\
&\quad + (4lm - 2l - 2m)(\sqrt{16})\\
&= 49.5692lm + 20.2871l + 12.2871m - 5.0953.
\end{aligned} \tag{13}$$

For $\alpha = (-1/2)$,

$$\begin{aligned}
R_{-1/2} &= \sum_{lm\in E(G)} \frac{1}{\sqrt{\mathfrak{L}(l)\times\mathfrak{L}(m)}}\\
&= (16)\left(\frac{1}{\sqrt{6}}\right) + (16l + 16m - 24)\left(\frac{1}{\sqrt{9}}\right)\\
&\quad + (12lm - 8l - 8m + 8)\left(\frac{1}{\sqrt{12}}\right)\\
&\quad + (4lm - 2l - 2m)\left(\frac{1}{\sqrt{16}}\right)\\
&= 3.9641lm + 3.0239l + 2.5239m + 0.8413.
\end{aligned} \tag{14}$$

□

Theorem 2. *Let $G \cong NbO$, with $l, m \geq 1$. Then, the atom bond connectivity index corresponds to*

$$\mathrm{ABC} = 10.1954lm + 4.2779l + 4.2779m + 0.4776. \quad (15)$$

Proof

$$\begin{aligned}\mathrm{ABC} &= \sum_{lm\in E(G)} \sqrt{\frac{\mathfrak{L}(l) + \mathfrak{L}(m) - 2}{\mathfrak{L}(l) \times \mathfrak{L}(m)}} \\ &= (16)\left(\sqrt{\frac{3}{6}}\right) + (16l + 16m - 24)\left(\sqrt{\frac{4}{9}}\right) \\ &\quad + (12lm - 8l - 8m + 8)\left(\sqrt{\frac{5}{12}}\right) \\ &\quad + (4lm - 2l - 2m)\left(\sqrt{\frac{6}{16}}\right) \\ &= 10.1954lm + 4.2779l + 4.2779m + 0.4776.\end{aligned} \quad (16)$$

□

Theorem 3. *Consider the graph of $G \cong NbO$ which has $l, m \geq 1$ and geometric arithmetic index is corresponding to the following:*

$$\mathrm{GA} = 15.8769lm + 6.0820l + 6.0820m - 0.4053. \quad (17)$$

Proof

$$\begin{aligned}\mathrm{GA} &= \sum_{lm\in E(G)} \frac{2\sqrt{\mathfrak{L}(l) \times \mathfrak{L}(m)}}{\mathfrak{L}(l) + \mathfrak{L}(m)} \\ &= (16)\left(\frac{2\sqrt{6}}{5}\right) + (16l + 16m - 24)\left(\frac{2\sqrt{9}}{6}\right) \\ &\quad + (12lm - 8l - 8m + 8)\left(\frac{2\sqrt{12}}{7}\right) \\ &\quad + (4lm - 2l - 2m)\left(\frac{2\sqrt{16}}{8}\right) \\ &= 15.8769lm + 6.0820l + 6.0820m - 0.4053.\end{aligned} \quad (18)$$

□

Theorem 4. *The forgotten index for the graph of $G \cong NbO[l, m]$ with $l, m \geq 1$ is corresponding to*

$$F = 428lm + 24l + 24m - 24. \quad (19)$$

Proof

$$\begin{aligned}F &= \sum_{lm\in E(G)} \left(\mathfrak{L}(l)^2 + \mathfrak{L}(m)^2\right) \\ &= (16)(13) + (16l + 16m - 24)(18) \\ &\quad + (12lm - 8l - 8m + 8)(25) + (4lm - 2l - 2m)(32) \\ &= 428lm + 24l + 24m - 24.\end{aligned} \quad (20)$$

□

Theorem 5. *The augmented index for the graph of $G \cong NbO[l, m]$ with $l, m \geq 1$ is corresponding to*

$$\mathrm{AZI} = 241.7398lm + 33.7320l + 33.7320m - 34.783. \quad (21)$$

Proof

$$\begin{aligned}\mathrm{AZI} &= \sum_{lm\in E(G)} \left(\frac{\mathfrak{L}(l) \times \mathfrak{L}(m)}{\mathfrak{L}(l) + \mathfrak{L}(m) - 2}\right)^3 \\ &= (16)\left(\frac{6}{3}\right)^3 + (16l + 16m - 24)\left(\frac{9}{4}\right)^3 \\ &\quad + (12lm - 8l - 8m + 8)\left(\frac{12}{5}\right)^3 \\ &\quad + (4lm - 2l - 2m)\left(\frac{16}{6}\right)^3 \\ &= 241.7398lm + 33.7320l + 33.7320m - 34.783.\end{aligned} \quad (22)$$

□

Theorem 6. *Consider the graph of $G \cong NbO[l, m]$ such that $l, m \geq 1$ and the first and second Zagreb index is corresponding to*

$$\begin{aligned}M_1 &= 116lm + 24l + 24m - 8, \\ M_2 &= 208lm + 16l + 16m - 24.\end{aligned} \quad (23)$$

Proof

$$\begin{aligned}M_1 &= \sum_{lm\in E(G)} \mathfrak{L}(l) + \mathfrak{L}(m) \\ &= (16)(5) + (16l + 16m - 24)(6) \\ &\quad + (12lm - 8l - 8m + 8)(7) + (4lm - 2l - 2m)(8) \\ &= 116lm + 24l + 24m - 8, \\ M_2 &= \sum_{lm\in E(G)} \mathfrak{L}(l) \times \mathfrak{L}(m) \\ &= (16)(6) + (16l + 16m - 24)(9) \\ &\quad + (12lm - 8l - 8m + 8)(12) + (4lm - 2l - 2m)(16) \\ &= 208lm + 16l + 16m - 24.\end{aligned} \quad (24)$$

□

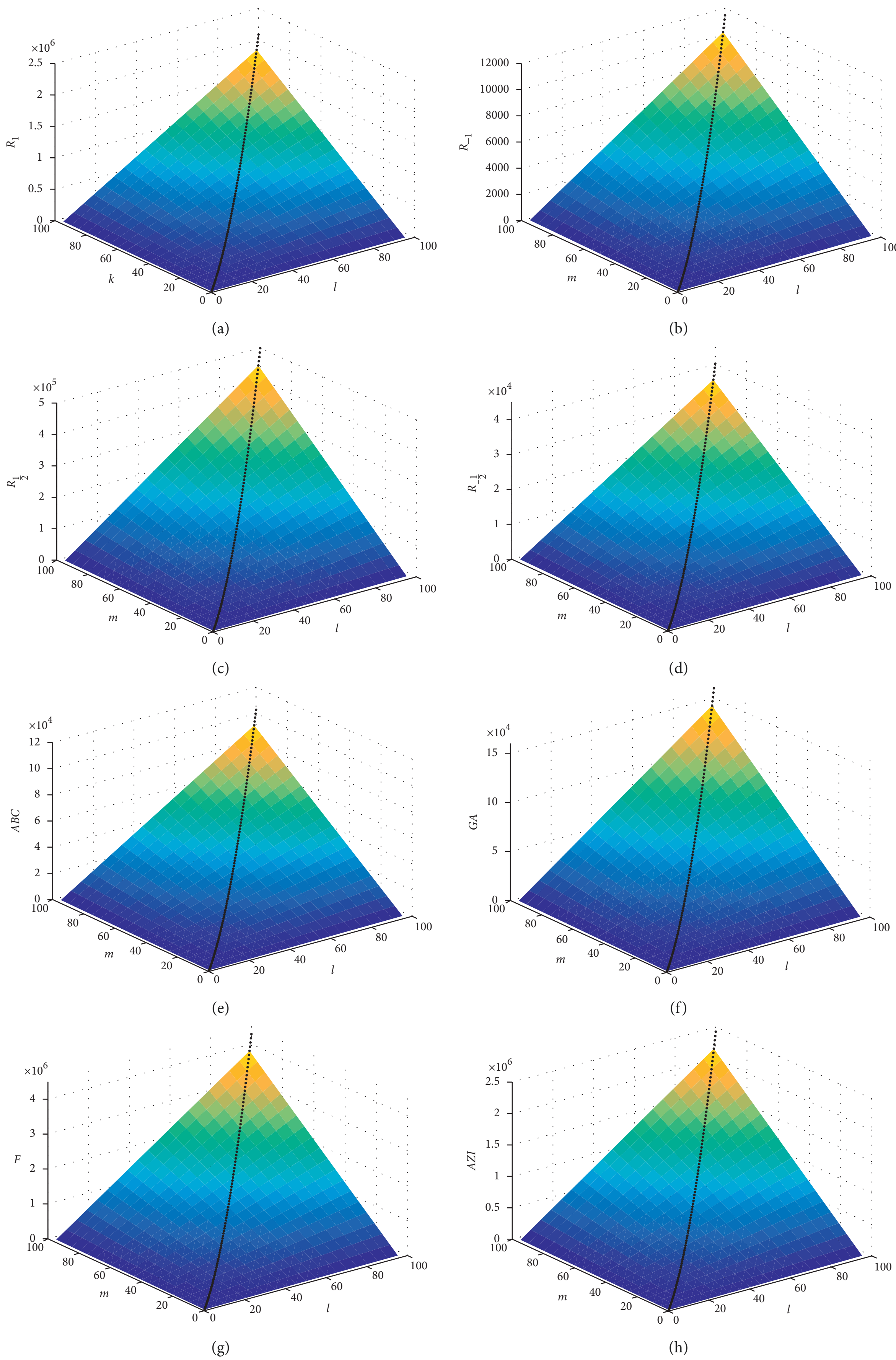

Figure 2: Continued.

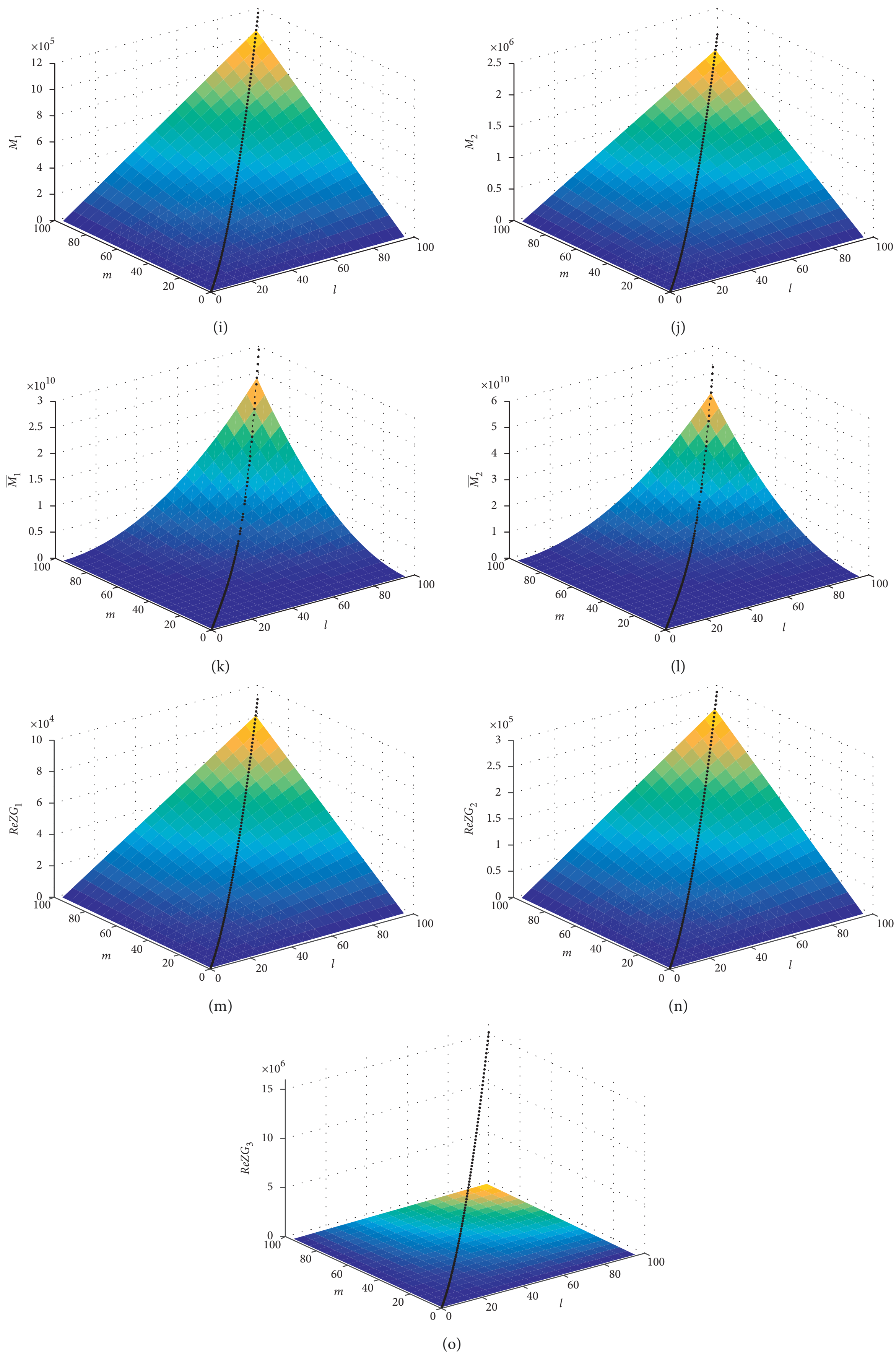

Figure 2: An interactive view of scattered plot together with surface plot of indices. (a) (m, n, R_1). (b) (m, n, R_{-1}). (c) $(m, n, R_{1/2})$. (d) $(m, n, R_{-1/2})$. (e) (m, n, ABC). (f) (m, n, GA). (g) (m, n, F). (h) (m, n, AZI). (i) (m, n, M_1). (j) (m, n, M_2). (k) $(m, n, \overline{M}_1)$. (l) $(m, n, \overline{M}_2)$. (m) (m, n, ReZG_1). (n) (m, n, ReZG_2). (o) (m, n, ReZG_3).

Table 3: Values of HoF and Entropy for units of NbO.

$[m, n]$	Units of frequency	HoF $\times 10^{-22}$ kJ	Entropy $\times 10^{-22}$Jmol^{-1}K^{-1}
[1, 1]	4	−26.9545	3.1949
[2, 2]	16	−107.8180	12.7798
[3, 3]	36	−242.5905	28.7545
[4, 4]	64	−431.2720	51.1192
[5, 5]	100	−673.8625	79.8737
[6, 6]	144	−970.3620	115.0182
[7, 7]	196	−1320.7705	156.5526

Theorem 7. *The first and second Zagreb coindices for the graph of* $(\mathscr{G}) \cong NbO[l, m]$ *with* $l, m \geq 1$ *are corresponding to*

$$\begin{aligned}\overline{M}_1 &= 288l^2m^2 + 268l^2m + 268lm^2 + 60l^2 \\ &\quad + 36lm + 60m^2 - 12l - 12m + 8, \\ \overline{M}_2 &= 512l^2m^2 + 384l^2m + 384lm^2 + 72l^2 \\ &\quad - 122lm + 72m^2 - 28l - 28m + 28.\end{aligned} \tag{25}$$

Proof

$$\begin{aligned}\overline{M}_1 &= \sum_{lm \notin E(G)} \mathfrak{L}(l) + \mathfrak{L}(m) \\ &= 2|E(G)|(|V(G)| - 1) - M_1 \\ &= 2(16lm + 6l + 6m)(9lm + 5l + 5m + 2 - 1) \\ &\quad - (116lm + 24l + 24m - 8) \\ &= 288l^2m^2 + 268l^2m + 268lm^2 + 60l^2 \\ &\quad + 36lm + 60m^2 - 12l - 12m + 8, \\ \overline{M}_2 &= \sum_{lm \notin E(G)} \mathfrak{L}(l) \times \mathfrak{L}(m) \\ &= 2|E(G)|^2 - \frac{1}{2}M_1 - M_2 \\ &= 2(16lm + 6l + 6m)^2 \\ &\quad - \frac{1}{2}(116lm + 24l + 24m - 8) \\ &\quad - (208lm + 16l + 16m - 24) \\ &= 512l^2m^2 + 384l^2m + 384lm^2 \\ &\quad + 72l^2 - 122lm + 72m^2 - 28l - 28m + 28.\end{aligned} \tag{26}$$

□

Theorem 8. *The redefined Zagreb indices for the graph of* $G \cong NbI[l, m]$ *with* $l, m \geq 1$ *correspond to*

$$\begin{aligned}\mathrm{ReZG}_1 &= 9lm + 5l + 5m + 2, \\ \mathrm{ReZG}_2 &= 28.5714lm + 6.2857l + 6.2857m - 3.0857, \\ \mathrm{ReZG}_3 &= 1520lm - 64l - 64m - 144.\end{aligned} \tag{27}$$

Proof

$$\begin{aligned}\mathrm{ReZG}_1 &= \sum_{lm \in E(G)} \frac{\mathfrak{L}(l) + \mathfrak{L}(m)}{\mathfrak{L}(l) \times \mathfrak{L}(m)} \\ &= (16)\left(\frac{5}{6}\right) + (16l + 16m - 24)\left(\frac{6}{9}\right) \\ &\quad + (12lm - 8l - 8m + 8)\left(\frac{7}{12}\right) \\ &\quad + (4lm - 2l - 2m)\left(\frac{8}{16}\right) \\ &= 9lm + 5l + 5m + 2, \\ \mathrm{ReZG}_2 &= \sum_{lm \in E(G)} \frac{\mathfrak{L}(l) \times \mathfrak{L}(m)}{\mathfrak{L}(l) + \mathfrak{L}(m)} \\ &= (16)\left(\frac{6}{5}\right) + (16l + 16m - 24)\left(\frac{9}{6}\right) \\ &\quad + (12lm - 8l - 8m + 8)\left(\frac{12}{7}\right) \\ &\quad + (4lm - 2l - 2m)\left(\frac{16}{8}\right) \\ &= 28.5714lm + 6.2857l + 6.2857m - 3.0857, \\ \mathrm{ReZG}_3 &= \sum_{lm \in E(G)} ((\mathfrak{L}(l) \times \mathfrak{L}(m))(\mathfrak{L}(l) + \mathfrak{L}(m))) \\ &= (16)(30) + (16l + 16m - 24)(54) \\ &\quad + (12lm - 8l - 8m + 8)(84) \\ &\quad + (4lm - 2l - 2m)(128) \\ &= 1520lm - 64l - 64m - 144.\end{aligned} \tag{28}$$

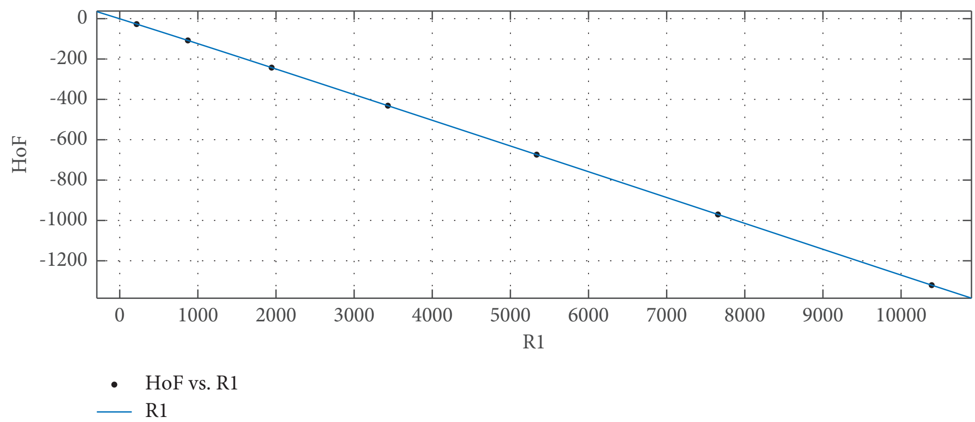

Figure 3: R_1 (x-axis) vs. HoF (y-axis).

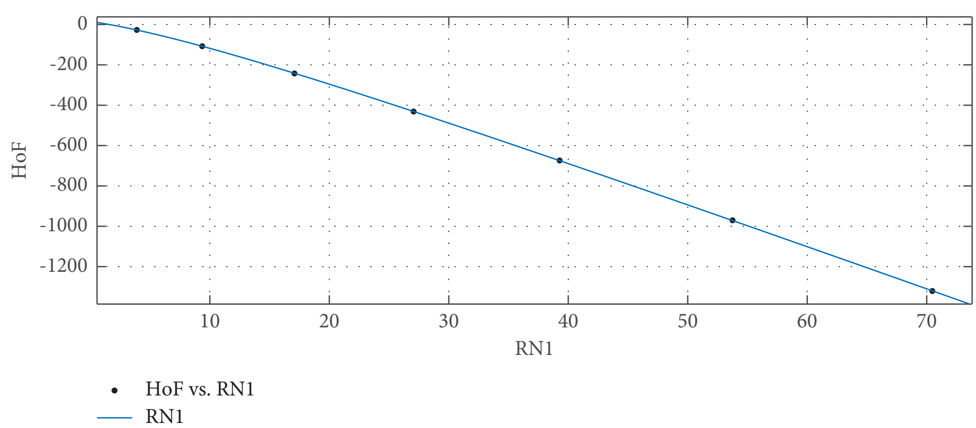

Figure 4: R_{-1} vs. HoF.

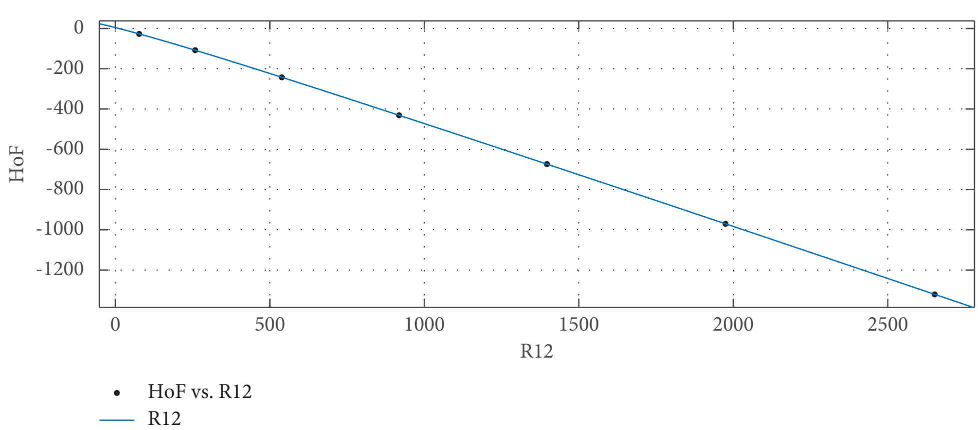

Figure 5: $R_{(1/2)}$ vs. HoF.

Graphical illustration for each index corresponding to $l = m = i; i = 1, 2, \ldots, 100$, computed above, is provided in Figure 2. □

2.1. Thermodynamical Properties (HoF and Entropy) of Niobium (II) Oxide. Many topological indices are derived for unit cell of NbO, including M_1; M_1; ABC; GA; and AZI.

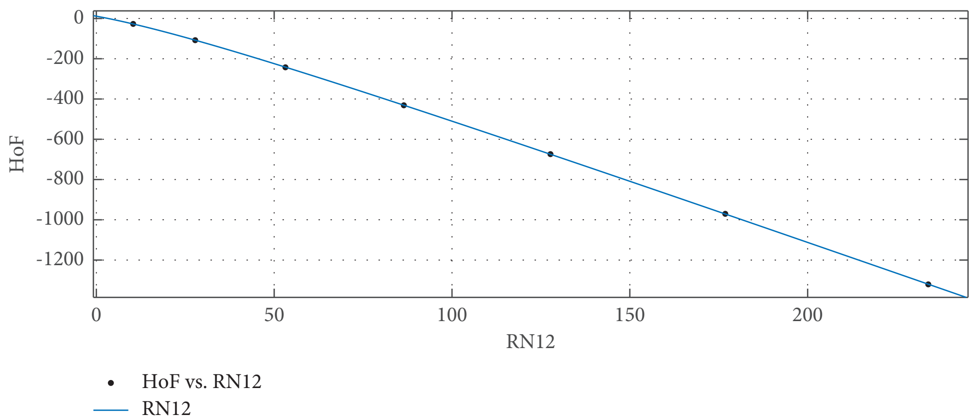

Figure 6: $R_{(-1/2)}$ vs. HoF.

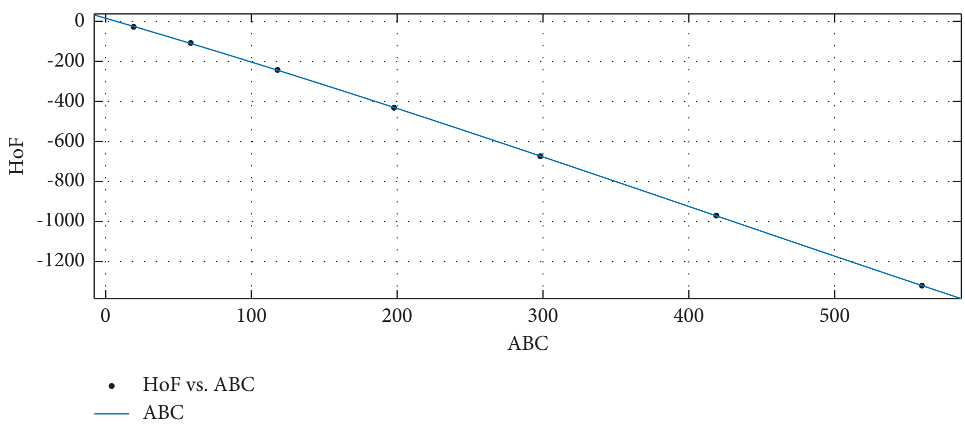

Figure 7: ABC vs. HoF.

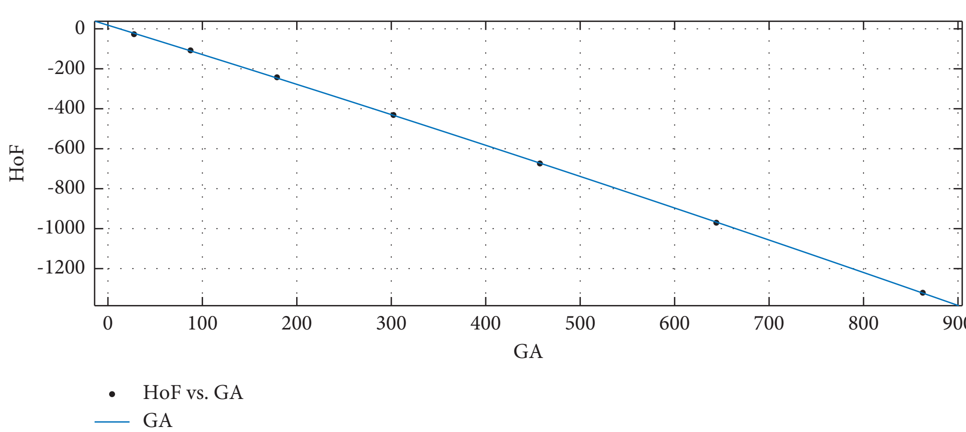

Figure 8: GA vs. HoF.

These indices are linked to thermodynamic properties of NbO, such as heat of formation (HoF) or enthalpy and entropy. The standard molar enthalpy and entropy of NbO is $-405.8\,\mathrm{kJmol}^{-1}$ and $48.1\mathrm{Jmol}^{-1}K^{-1}$, respectively. Table 3 represents the numerical values of HoF and Entropy.

2.2. Statistical Models for HoF and Topological Indices. In this section, mathematical frameworks are created for the topological index (computed in Section 2) and HoF (given in Section 2.1) of NbO. All fitted curves are shown in Figures 3–17 and also the constant quantity values of the

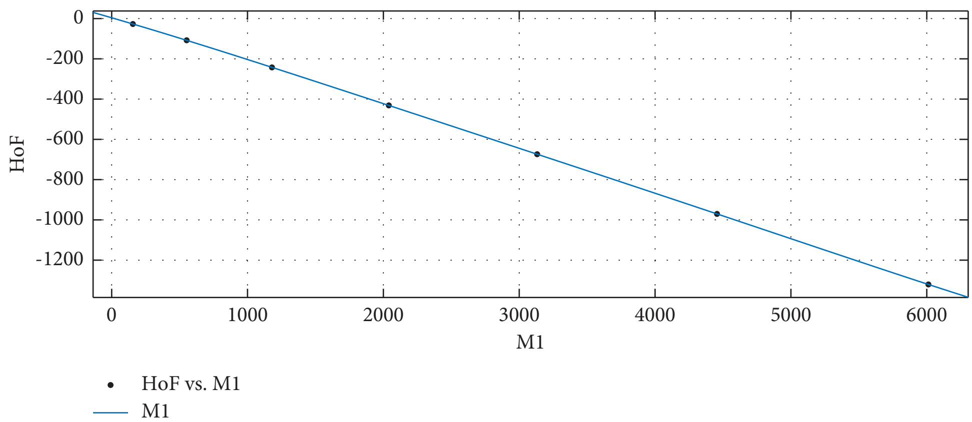

FIGURE 9: M_1 vs. HoF.

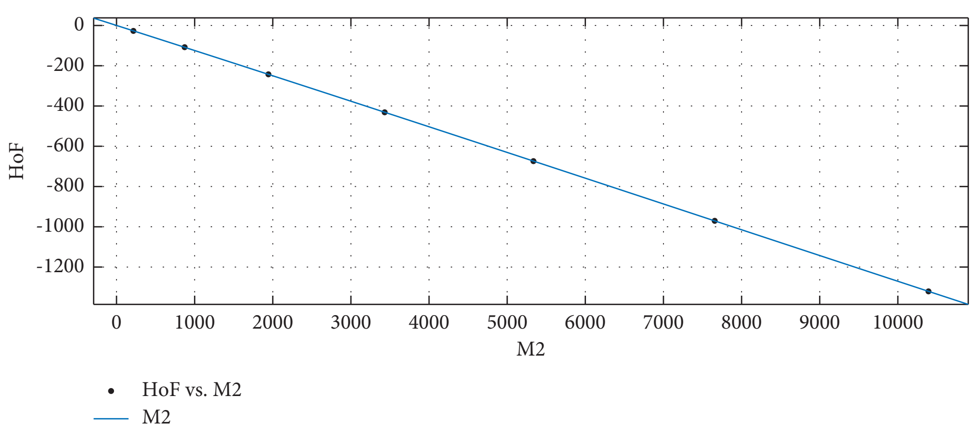

FIGURE 10: M_2 vs. HoF.

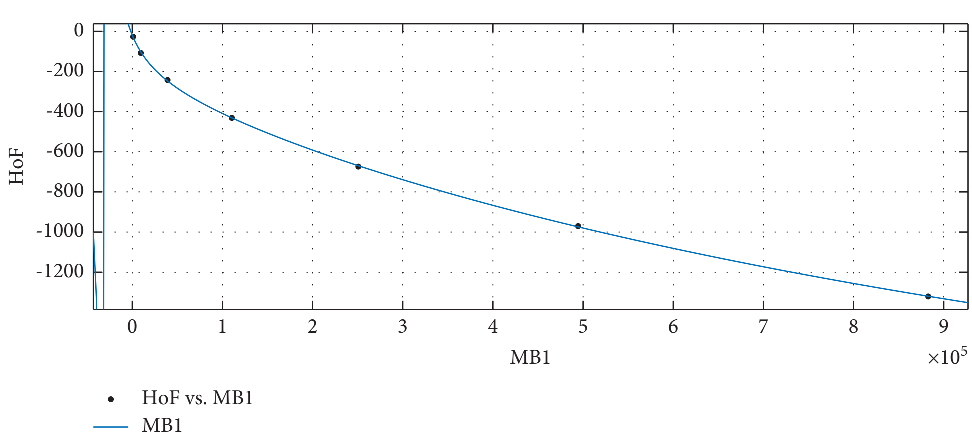

FIGURE 11: $\overline{M}_1$ vs. HoF.

fitted curves are depicted in Tables 4–18. Also, the goodness of fit for indices vs. HoF for NbO is depicted in Table 19. Let ε and γ denote the mean and standard deviation that is used to rescale the data.

(i) Estimation of rational polynomial for HoF vs. R_1 is

$$\mathrm{HoF}(x) = \frac{p_1 x + p_2}{x^4 + q_1 x^3 + q_2 x^2 + q_3 x + q_4}, \tag{29}$$

where $x = R_1$ is rescaled through $\varepsilon = 4264$ and $\gamma = 3746$.

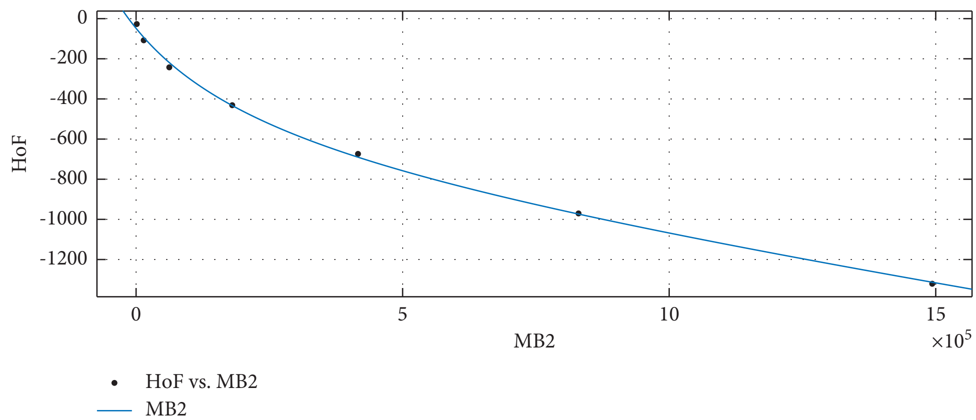

FIGURE 12: $\overline{M}_2$ vs. HoF.

(ii) Estimation of rational polynomial for HoF vs. R_{-1} is

$$\text{HoF}(x) = \frac{p_1x^2 + p_2x + p_3}{x^2 + q_1x + q_2}, \quad (30)$$

where $x = R_{-1}$ is rescaled through $\varepsilon = 31.56$ and $\gamma = 24.34$.

(iii) Estimation of rational polynomial for HoF vs. $R_{1/2}$ is

$$\text{HoF}(x) = \frac{p_1x^2 + p_2x + p_3}{x^3 + q_1x^2 + q_2x + q_3}, \quad (31)$$

where $x = R_{(1/2)}$ rescaled through $\varepsilon = 1117$ and $\gamma = 945.4$.

(iv) Estimation of rational polynomial for HoF vs. $R_{(-1/2)}$ is

$$\text{HoF}(x) = \frac{p_1x^2 + p_2x + p_3}{x^2 + q_1x + q_2}, \quad (32)$$

where $x = R_{(-1/2)}$ is rescaled through $\varepsilon = 102.3$ and $\gamma = 81.85$.

(v) Estimation of rational polynomial for HoF vs. ABC is

$$\text{HoF}(x) = \frac{p_1x + p_2}{x^2 + q_1x + q_2}, \quad (33)$$

where $x = \text{ABC}$ is rescaled through $\varepsilon = 238.6$ and $\gamma = 198.4$.

(vi) Estimation of rational polynomial for HoF vs. GA is

$$\text{HoF}(x) = \frac{p_1x^2 + p_2x + p_3}{x + q_1}, \quad (34)$$

where $x = \text{GA}$ is rescaled through $\varepsilon = 365.8$ and $\gamma = 306.5$.

(vii) Estimation of rational polynomial for HoF vs. M_1 is

$$\text{HoF}(x) = \frac{p_1x + p_2}{x^4 + q_1x^3 + q_2x^2 + q_3x + q_4}, \quad (35)$$

where $x = M_1$ is rescaled through $\varepsilon = 2504$ and $\gamma = 2153$.

(viii) Estimation of rational polynomial for HoF vs. M_2 is

$$\text{HoF}(x) = \frac{p_1x + p_2}{x^3 + q_1x^2 + q_2x + q_3}, \quad (36)$$

where $x = M_2$ is rescaled through $\varepsilon = 4264$ and $\gamma = 3746$.

(ix) Estimation of rational polynomial for HoF vs. $\overline{M}_1$ is

$$\text{HoF}(x) = \frac{p_1x^2 + p_2x + p_3}{x^2 + q_1x + q_2}, \quad (37)$$

where $x = \overline{M}_1$ is rescaled through $\varepsilon = 2.554e + 05$ and $\gamma = 3.276e + 05$.

(x) Estimation of rational polynomial for HoF vs. $\overline{M}_2$ is

$$\text{HoF}(x) = \frac{p_1x^2 + p_2x + p_3}{x^2 + q_1x + q_2}, \quad (38)$$

where $x = \overline{M}_2$ is rescaled through $\varepsilon = 4.283e + 05$ and $\gamma = 5.545e + 05$.

(vi) Estimation of rational polynomial for HoF vs. AZI is

$$\text{HoF}(x) = \frac{p_1x^2 + p_2x + p_3}{x + q_1}, \quad (39)$$

where $x = \text{AZI}$ is rescaled through $\varepsilon = 1818$ and $\gamma = 1625$.

(vii) Estimation of rational polynomial for HoF vs. F is

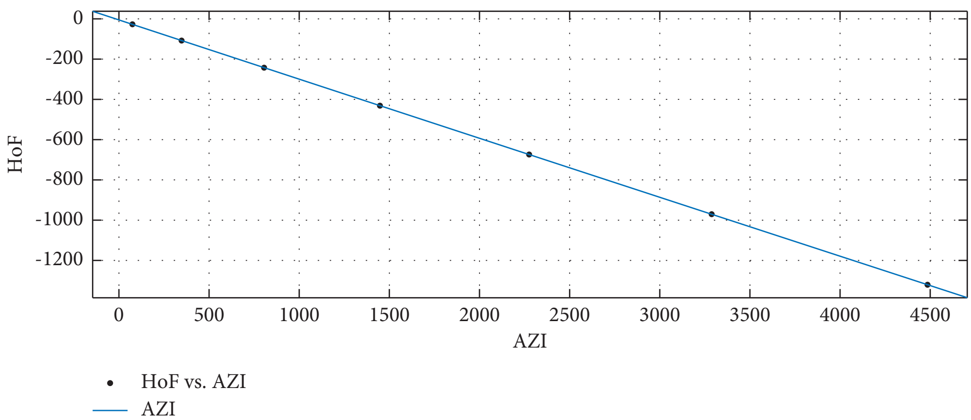

Figure 13: AZI vs. HoF.

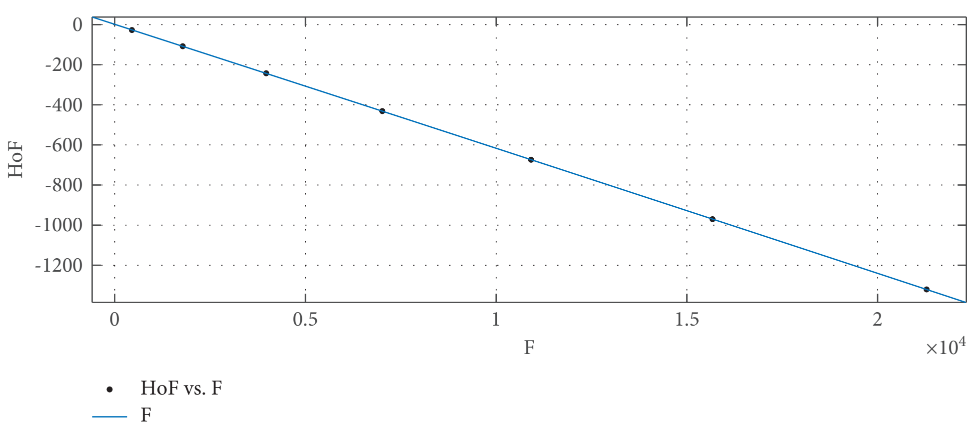

Figure 14: F vs. HoF.

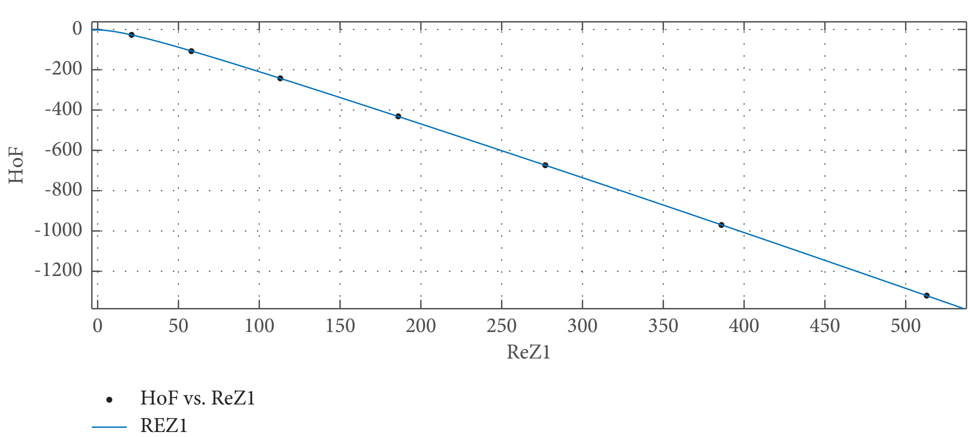

Figure 15: $ReZG_1$ vs. HoF.

$$\mathrm{HoF}(x) = \frac{p_1 x^2 + p_2 x + p_3}{x + q_1}, \tag{40}$$

where $x = F$ is rescaled through $\varepsilon = 8728$ and $\gamma = 7669$.

(viii) Estimation of rational polynomial for HoF vs. $ReZG_1$ is

$$\mathrm{HoF}(x) = \frac{p_1 x^2 + p_2 x + p_3}{x^3 + q_1 x^2 + q_2 x + q_3}, \tag{41}$$

where $x = ReZG_1$ is rescaled through $\varepsilon = 222$ and $\gamma = 180.3$.

(ix) Estimation of rational polynomial for HoF vs. $ReZG_2$ is

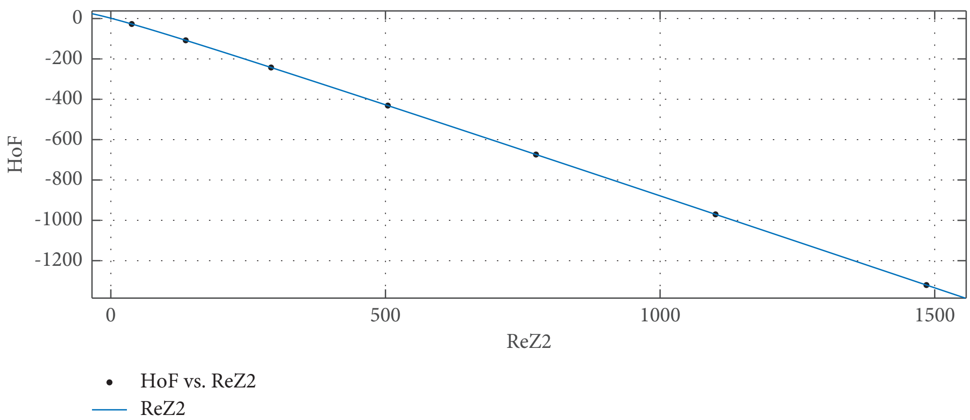

FIGURE 16: $ReZG_2$ vs. HoF.

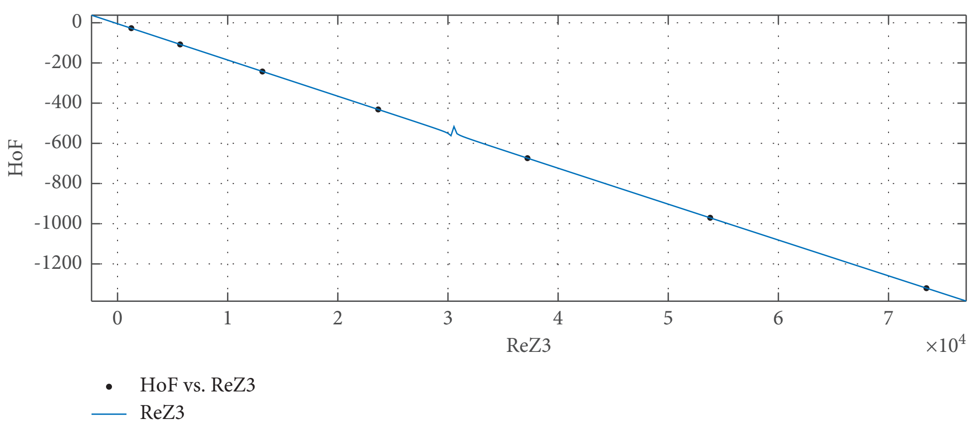

FIGURE 17: $ReZG_3$ vs. HoF.

TABLE 4: R_1 vs. HoF.

	p_i	Confidence interval (CI)	q_i	CI
$i = 1$	$-2.089e+05$	$(-1.39e+06,\ 9.72e+05)$	-3.028	$(-8.911,\ 2.856)$
$i = 2$	$-2.381e+05$	$(-1.583e+06,\ 1.107e+06)$	3.559	$(-15.22,\ 22.34)$
$i = 3$	—	—	-4.613	$(-33.85,\ 24.62)$
$i = 4$	—	—	443.2	$(-2061,\ 2947)$

TABLE 5: R_{-1} vs. HoF.

	p_i	CI	q_i	CI
$i = 1$	$-3.496e+07$	$(-1.177e+11,\ 1.176e+11)$	$6.704e+04$	$(-2.255e+08,\ 2.257e+08)$
$i = 2$	$-9.916e+07$	$(-3.337e+11,\ 3.335e+11)$	$1.33e+05$	$(-4.473e+08,\ 4.476e+08)$
$i = 3$	$-6.91e+07$	$(-2.325e+11,\ 2.324e+11)$	—	—

$$\mathrm{HoF}(x) = \frac{p_1 x^2 + p_2 x + p_3}{x^3 + q_1 x^2 + q_2 x + q_3}, \qquad (42)$$

where $x = \mathrm{ReZG}_2$ is rescaled through $\varepsilon = 618.6$ and $\gamma = 531.8$.

(x) Estimation of rational polynomial for HoF vs. ReZG_3 is

$$\mathrm{HoF}(x) = \frac{p_1 x^2 + p_2 x + p_3}{x^2 + q_1 x + q_2}, \qquad (43)$$

Table 6: $R_{(1/2)}$ vs. HoF.

	p_i	CI	q_i	CI
$i = 1$	$3.108e+07$	$(-6.357e+10,\ 6.364e+10)$	229.4	$(-4.749e+05,\ 4.753e+05)$
$i = 2$	$8.362e+07$	$(-1.71e+11,\ 1.711e+11)$	$-6.361e+04$	$(-1.302e+08,\ 1.301e+08)$
$i = 3$	$5.528e+07$	$(-1.13e+11,\ 1.131e+11)$	$-1.04e+05$	$(-2.128e+08,\ 2.126e+08)$

Table 7: $R_{(-1/2)}$ vs. HoF.

	p_i	CI	q_i	CI
$i = 1$	$-3.55e+07$	$(-9.978e+10,\ 9.971e+10)$	$6.963e+04$	$(-1.956e+08,\ 1.957e+08)$
$i = 2$	$-9.948e+07$	$(-2.796e+11,\ 2.794e+11)$	$1.305e+05$	$(-3.666e+08,\ 3.668e+08)$
$i = 3$	$-6.838e+07$	$(-1.921e+11,\ 1.92e+11)$	—	—

Table 8: ABC vs. HoF.

	p_i	CI	q_i	CI
$i = 1$	$-3.504e+04$	$(-6.796e+04,\ -2111)$	-3.75	$(-5.523,\ -1.977)$
$i = 2$	$-4.081e+04$	$(-7.88e+04,\ -2822)$	77.34	$(5.61,\ 149.1)$

Table 9: GA vs. HoF.

	p_i	CI	q_i	CI
$i = 1$	$4.637e+05$	$(-2.16e+10,\ 2.16e+10)$	$-4.433e+04$	$(-2.063e+09,\ 2.063e+09)$
$i = 2$	$2.091e+07$	$(-9.735e+11,\ 9.736e+11)$	—	—
$i = 3$	$2.35e+07$	$(-1.094e+12,\ 1.094e+12)$	—	—

Table 10: M_1 vs. HoF.

	p_i	CI	q_i	CI
$i = 1$	$-8.239e+04$	$(-5.395e+05,\ 3.747e+05)$	-3.054	$(-8.908,\ 2.8)$
$i = 2$	$-9.506e+04$	$(-6.215e+05,\ 4.314e+05)$	3.673	$(-15.16,\ 22.51)$
$i = 3$	—	—	-4.831	$(-34.56,\ 24.9)$
$i = 4$	—	—	177.9	$(-807.8,\ 1164)$

where $x = \mathrm{ReZG}_3$ is rescaled through $\varepsilon = 2.974e+04$ and $\gamma = 2.661e+04$.

2.3. Statistical Models for Entropy and Topological Indices. In this section, mathematical frameworks for the topological index (computed in Section 2) and Entropy (given in Section 2.1) of NbO are shown. All fitted curves are shown in Figures 18–32, and the parametric values of the fitted curves are given in Tables 20–34. Also, the goodness of fit for indices vs. entropy for NbO is depicted in Table 35.

(i) Estimated rational polynomial of Entropy vs. R_1 is

$$\text{Entropy}(x) = \frac{p_1 x + p_2}{x^3 + q_1 x^2 + q_2 x + q_3}, \tag{44}$$

where $x = R_1$ is rescaled through $\varepsilon = 4264$ and $\gamma = 3746$.

(ii) Estimated rational polynomial of Entropy vs. R_{-1} is

$$\text{Entropy}(x) = \frac{p_1 x^2 + p_2 x + p_3}{x^3 + q_1 x^2 + q_2 x + q_3}, \tag{45}$$

where $x = R_{-1}$ is rescaled through $\varepsilon = 31.56$ and $\gamma = 24.34$.

(iii) Estimated rational polynomial of Entropy vs. $R_{1/2}$ is

Table 11: M_2 vs. HoF.

	p_i	CI	q_i	CI
$i = 1$	$-7.613e+07$	$(-9.059e+10, 9.044e+10)$	442.4	$(-5.281e+05, 5.29e+05)$
$i = 2$	$-8.664e+07$	$(-1.031e+11, 1.029e+11)$	−1634	$(-1.945e+06, 1.942e+06)$
$i = 3$	—	—	$1.614e+05$	$(-1.917e+08, 1.921e+08)$

Table 12: $\overline{M}_1$ vs. HoF.

	p_i	CI	q_i	CI
$i = 1$	−3053	(−4237, −1869)	6.184	(2.407, 9.962)
$i = 2$	−6405	$(-1.054e+04, -2273)$	4.651	(0.886, 8.417)
$i = 3$	−3146	(−5686, −606.9)	—	—

Table 13: $\overline{M}_2$ vs. HoF.

	p_i	CI	q_i	CI
$i = 1$	$1.765e+07$	$(-2.879e+12, 2.879e+12)$	$-7.947e+04$	$(-1.296e+10, 1.296e+10)$
$i = 2$	$1.026e+08$	$(-1.673e+13, 1.673e+13)$	$-1.008e+05$	$(-1.644e+10, 1.644e+10)$
$i = 3$	$7.063e+07$	$(-1.152e+13, 1.152e+13)$	—	—

Table 14: AZI vs. HoF.

	p_i	CI	q_i	CI
$i = 1$	−8568	$(-1.056e+08, 1.056e+08)$	$-1.092e+04$	$(-1.426e+08, 1.425e+08)$
$i = 2$	$5.208e+06$	$(-6.799e+10, 6.8e+10)$	—	—
$I = 3$	$5.894e+06$	$(-7.693e+10, 7.694e+10)$	—	—

Table 15: F vs. HoF.

	p_i	CI	q_i	CI
$i = 1$	$2.344e+04$	$(-4.068e+08, 4.069e+08)$	$-1.46e+04$	$(-2.484e+08, 2.484e+08)$
$i = 2$	$6.948e+06$	$(-1.182e+11, 1.182e+11)$	—	—
$i = 3$	$7.852e+06$	$(-1.336e+11, 1.336e+11)$	—	—

Table 16: $ReZG_1$ vs. HoF.

	p_i	CI	q_i	CI
$i = 1$	$4.092e+07$	$(-4.611e+11, 4.611e+11)$	1129	$(-1.274e+07, 1.275e+07)$
$i = 2$	$1.012e+08$	$(-1.14e+12, 1.14e+12)$	$-8.418e+04$	$(-9.487e+08, 9.485e+08)$
$i = 3$	$6.262e+07$	$(-7.054e+11, 7.056e+11)$	$-1.188e+05$	$(-1.339e+09, 1.338e+09)$

Table 17: $ReZG_2$ vs. HoF.

	p_i	CI	q_i	CI
$i = 1$	$-4.999e+05$	$(-1.692e+06, 6.922e+05)$	−5.973	(−14.18, 2.234)
$i = 2$	$-1.264e+06$	$(-4.372e+06, 1.845e+06)$	1037	(−1429, 3503)
$i = 3$	$-7.929e+05$	$(-2.795e+06, 1.209e+06)$	1486	(−2265, 5236)

Table 18: $ReZG_3$ vs. HoF.

	p_i	CI	q_i	CI
$i = 1$	$-1.746e+05$	$(-4.898e+05,\ 1.407e+05)$	364.5	$(-298.9,\ 1028)$
$i = 2$	$-1.921e+05$	$(-9.603e+05,\ 5.761e+05)$	-10.06	$(-976,\ 955.8)$
$i = 3$	5470	$(-5.163e+05,\ 5.272e+05)$	—	—

Table 19: Goodness of fit for nidices vs. HoF for NbO.

Index	Fit type	SSE	R^2	Adjusted R^2	RMSE
R_1	rat14	0.02675	1	1	0.1636
R_{-1}	rat22	4.062	1	1	1.425
$R_{1/2}$	rat23	0.0617	1	1	0.2484
$R_{-1/2}$	rat22	3.122	1	1	1.249
ABC	rat12	15.19	1	1	2.25
GA	rat21	61.11	1	0.9999	4.513
M_1	rat14	0.1551	1	1	0.3938
M_2	rat13	0.7451	1	1	0.6104
$\overline{M}_1$	rat22	92.31	0.9999	0.9998	6.794
$\overline{M}_2$	rat22	1769	0.9987	0.9961	29.74
HM	rat13	0.123	1	1	0.248
AZI	rat21	0.3795	1	1	0.3557
F	rat21	1.776	1	1	0.7695
$ReZG_1$	rat23	2.238	1	1	1.496
$ReZG_2$	rat23	0.0005708	1	1	0.02389
$ReZG_3$	rat22	0.8455	1	1	0.6502

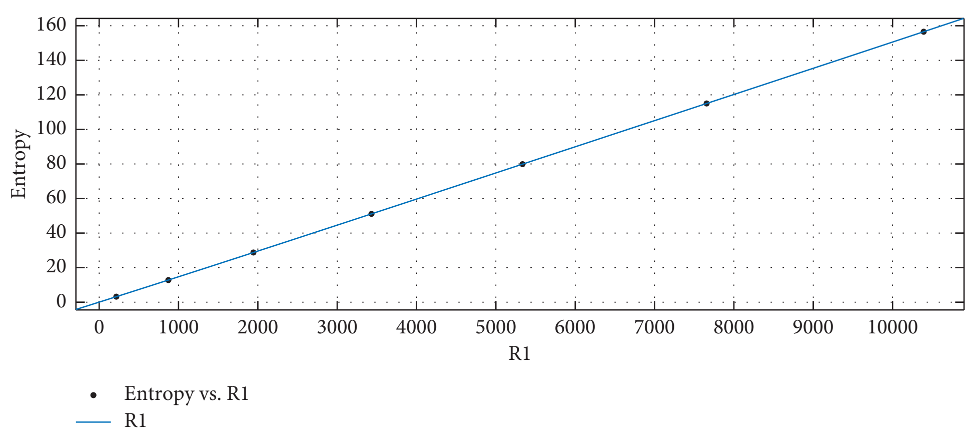

Figure 18: R_1 (x-axis) vs. Entropy (y-axis).

$$\text{Entropy}(x) = \frac{p_1x^2 + p_2x + p_3}{x^3 + q_1x^2 + q_2x + q_3}, \quad (46)$$

where $x = R_{1/2}$ is rescaled through $\varepsilon = 1117$ and $\gamma = 945.4$.

(iv) Estimated rational polynomial of Entropy vs. $R_{-1/2}$ is

$$\text{Entropy}(x) = \frac{p_1x^2 + p_2x + p_3}{x^3 + q_1x^2 + q_2x + q_3}, \quad (47)$$

where $x = R_{-1/2}$ is rescaled through $\varepsilon = 102.3$ and $\gamma = 81.85$.

(v) Estimated rational polynomial of Entropy vs. ABC is

$$\text{Entropy}(x) = \frac{p_1x^2 + p_2x + p_3}{x^3 + q_1x^2 + q_2x + q_3}, \quad (48)$$

where $x = \text{ABC}$ is rescaled through $\varepsilon = 238.6$ and $\gamma = 198.4$.

(vi) Estimated rational polynomial of Entropy vs. GA is

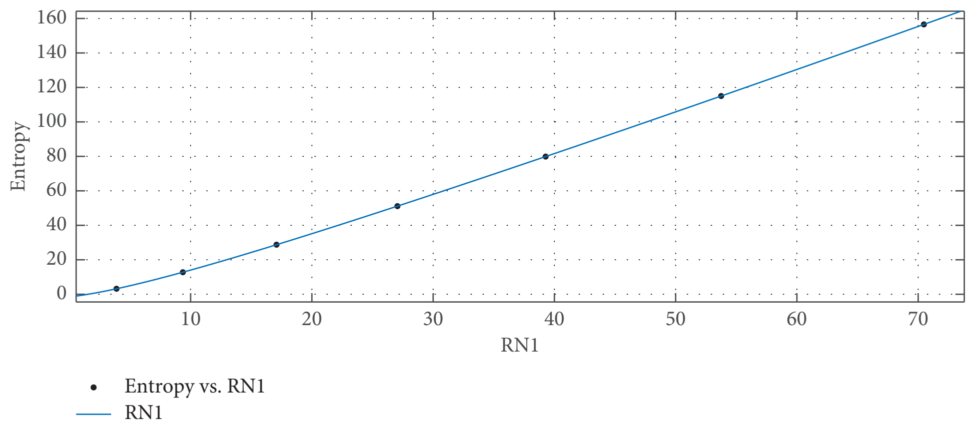

FIGURE 19: R_{-1} vs. Entropy.

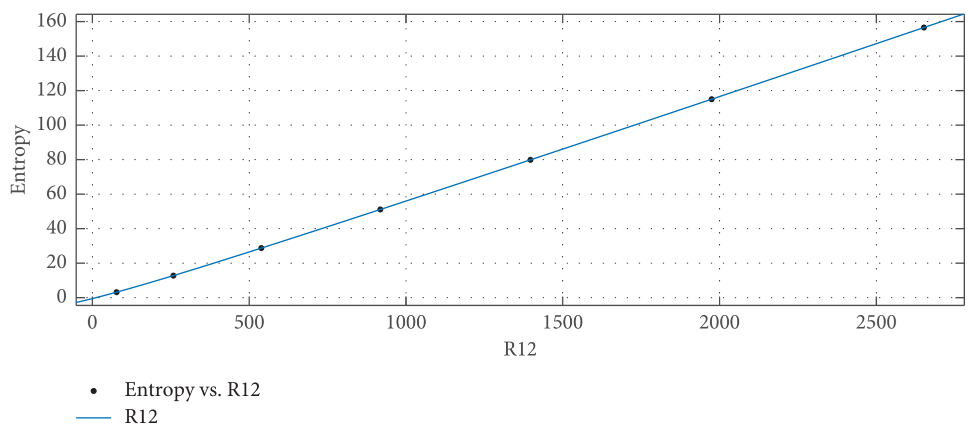

FIGURE 20: $R_{1/2}$ vs. Entropy.

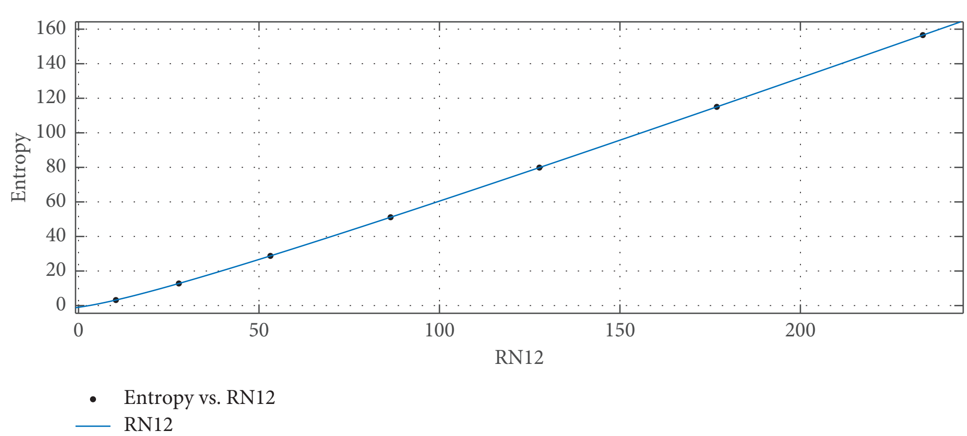

FIGURE 21: $R_{-1/2}$ vs. Entropy.

$$\text{Entropy}(x) = \frac{p_1 x + p_2}{x^3 + q_1 x^2 + q_2 x + q_3}, \quad (49)$$

where $x = \text{GA}$ is rescaled through $\varepsilon = 365.8$ and $\gamma = 306.5$.

(vii) Estimated rational polynomial of Entropy vs. M_1 is

$$\text{Entropy}(x) = \frac{p_1 x + p_2}{x^4 + q_1 x^3 + q_2 x^2 + q_3 x + q_4}, \quad (50)$$

where $x = M_1$ is rescaled through $\varepsilon = 2504$ and $\gamma = 2153$.

(viii) Estimated rational polynomial of Entropy vs. M_2 is

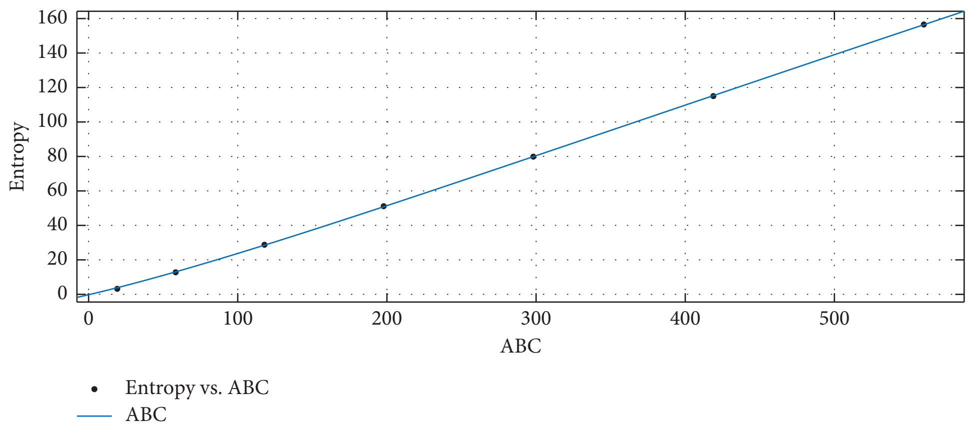

FIGURE 22: ABC vs. Entropy.

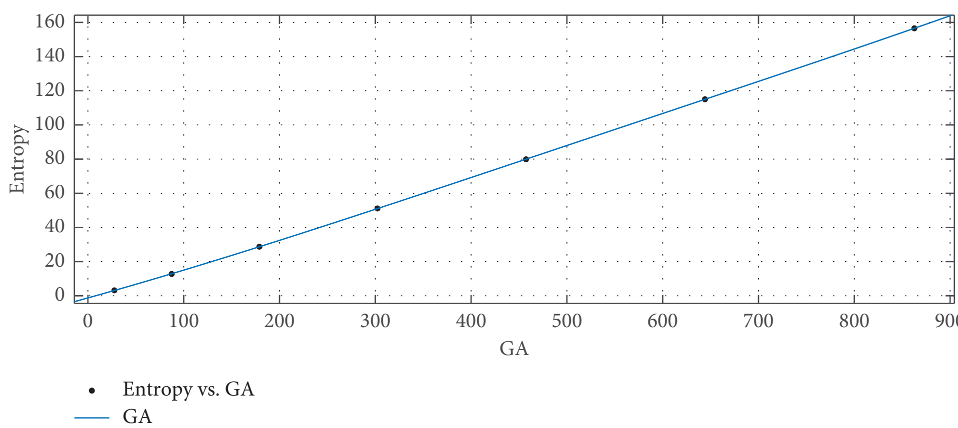

FIGURE 23: GA vs. Entropy.

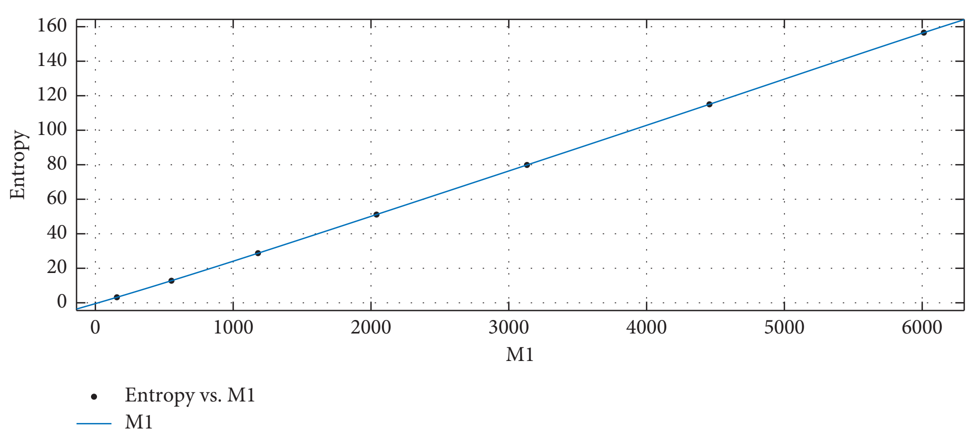

FIGURE 24: M_1 vs. Entropy.

$$\text{Entropy}(x) = \frac{p_1 x + p_2}{x^2 + q_1 x + q_2}, \tag{51}$$

where $x = M_2$ is rescaled through $\varepsilon = 4264$ and $\gamma = 3746$.

(ix) Estimated rational polynomial of Entropy vs. $\overline{M}_1$ is

$$\text{Entropy}(x) = \frac{p_1 x + p_2}{x^3 + q_1 x^2 + q_2 x + q_3}, \tag{52}$$

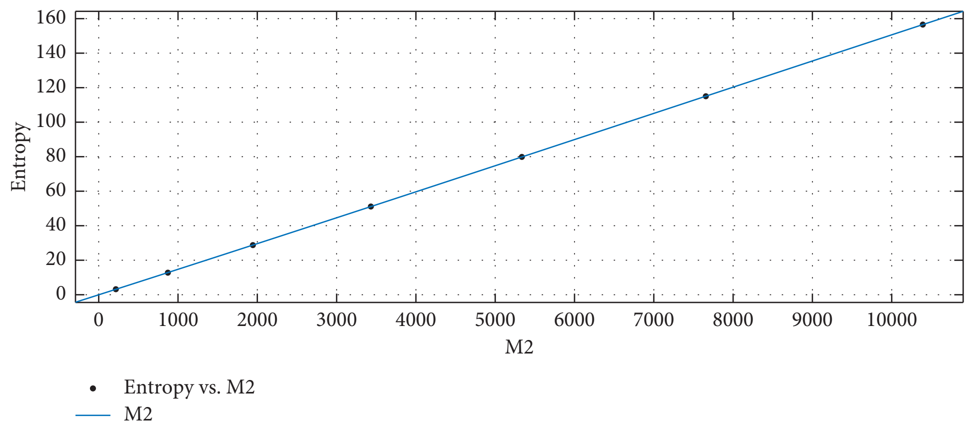

Figure 25: M_2 vs. Entropy.

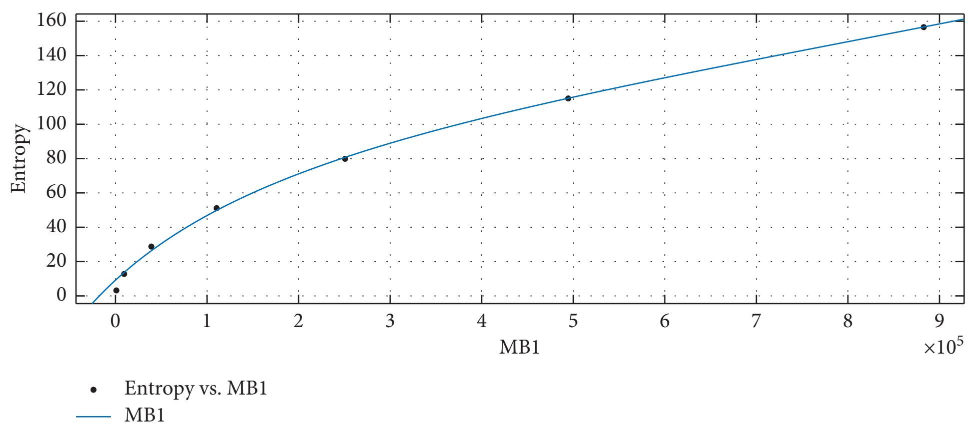

Figure 26: $\overline{M}_1$ vs. Entropy.

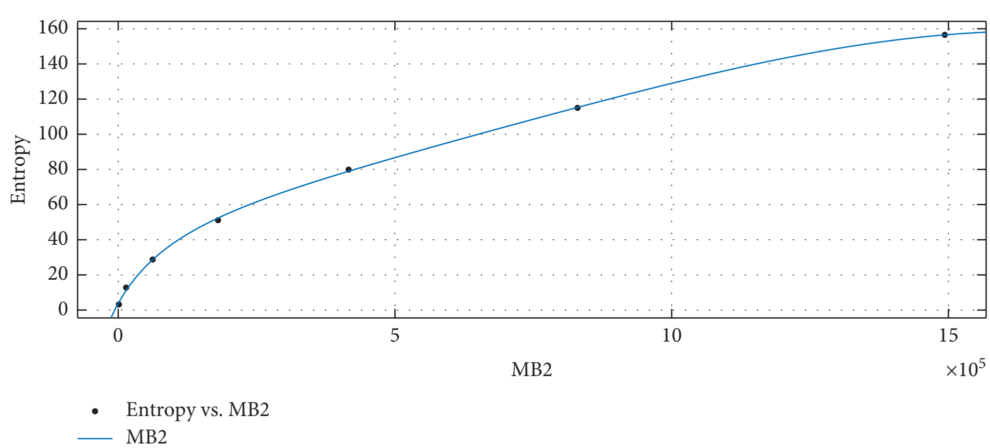

Figure 27: $\overline{M}_2$ vs. Entropy.

where $x = \overline{M}_1$ is rescaled through $\varepsilon = 2.554e + 05$ and $\gamma = 3.276e + 05$.

(x) Estimated rational polynomial of Entropy vs. $\overline{M}_2$ is

$$\text{Entropy}(x) = \frac{p_1 x + p_2}{x^4 + q_1 x^3 + q_2 x^2 + q_3 x + q_4}, \tag{53}$$

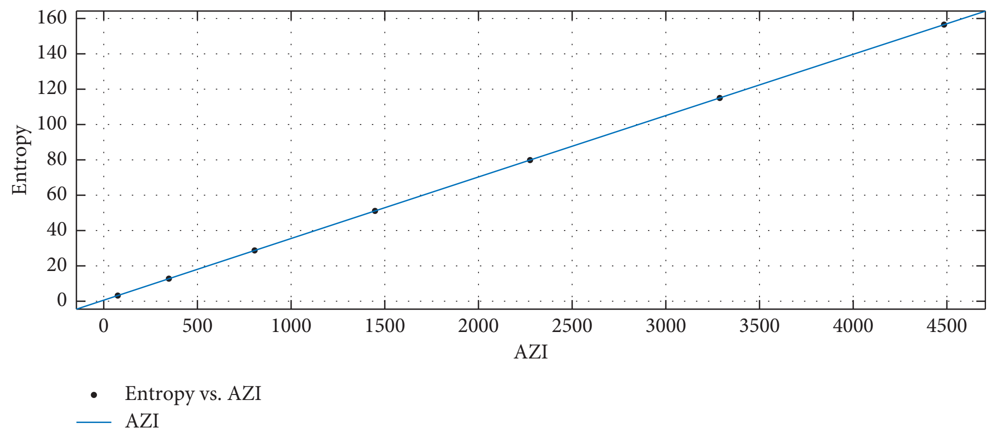

Figure 28: AZI vs. Entropy.

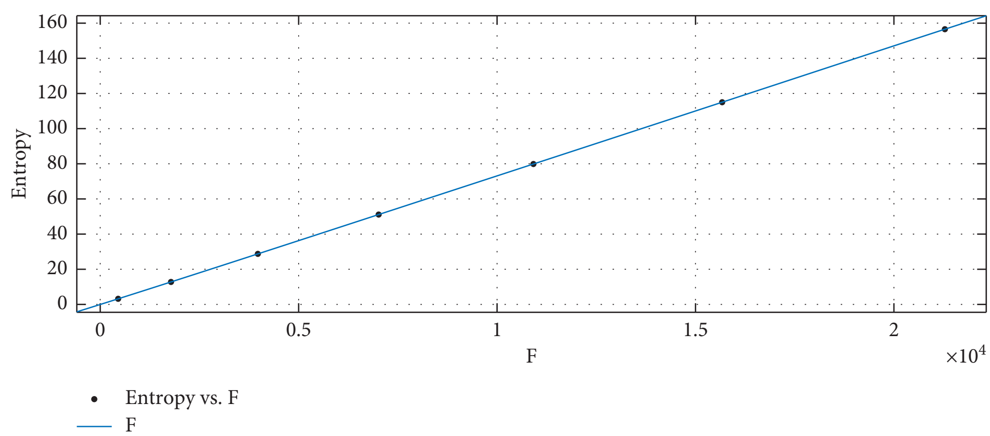

Figure 29: F vs. Entropy.

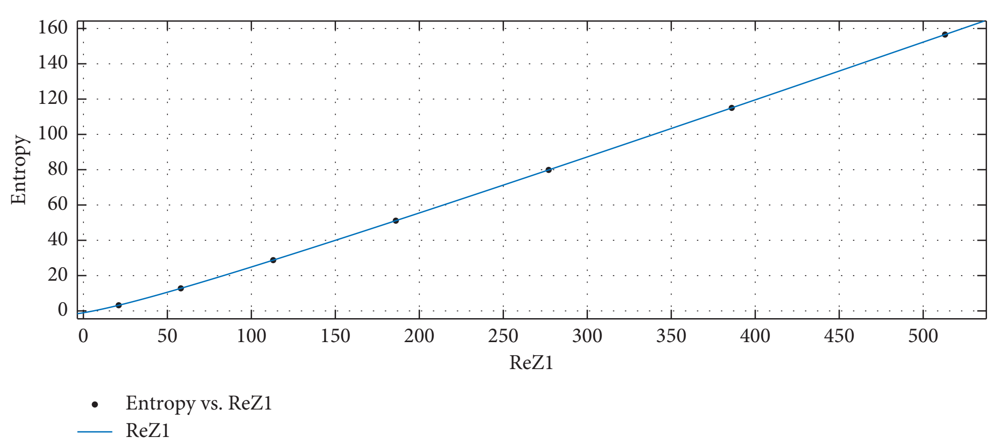

Figure 30: ReZG_1 vs. Entropy.

where $x = \overline{M}_2$ is rescaled through $\varepsilon = 4.283e + 05$ and $\gamma = 5.545e + 05$.

(xi) Estimated rational polynomial of Entropy vs. AZI is

$$\text{Entropy}(x) = \frac{p_1 x + p_2}{x^2 + q_1 x + q_2}, \tag{54}$$

where $x = \text{AZI}$ is rescaled through $\varepsilon = 1818$ and $\gamma = 1625$.

(xii) Estimated rational polynomial of Entropy vs. F is

$$\text{Entropy}(x) = \frac{p_1 x + p_2}{x^4 + q_1 x^3 + q_2 x^2 + q_3 x + q_4}, \tag{55}$$

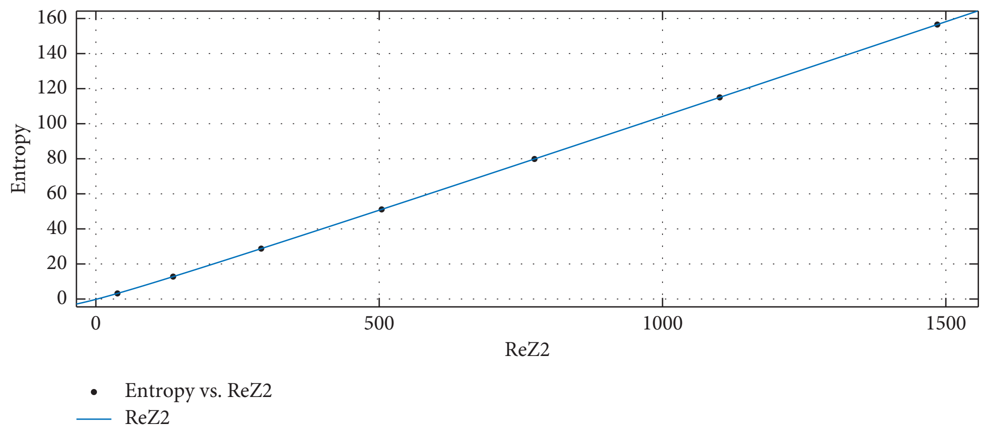

FIGURE 31: $ReZG_2$ vs. Entropy.

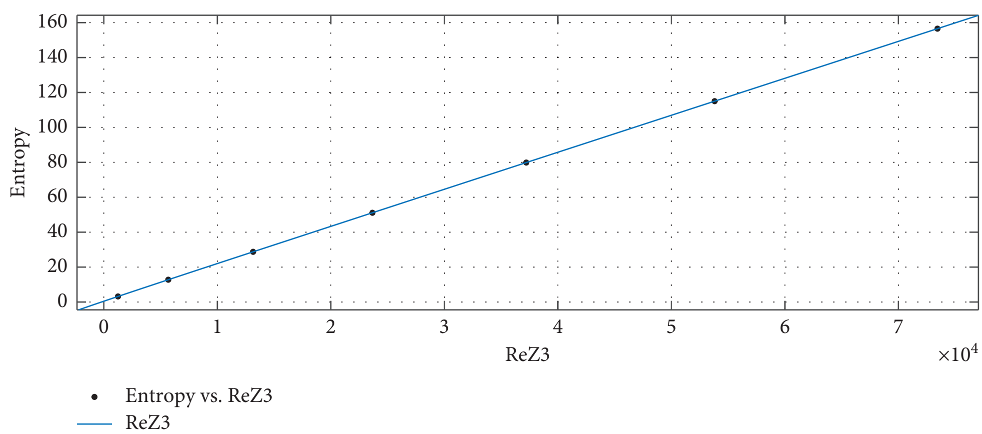

FIGURE 32: $ReZG_3$ vs. Entropy.

TABLE 20: R_1 vs. Entropy.

	p_i	CI	q_i	CI
$i = 1$	$-2.646e + 04$	$(-6.984e + 04,\ 1.691e + 04)$	-3.384	$(-5.642,\ -1.127)$
$i = 2$	$-3.014e + 04$	$(-7.949e + 04,\ 1.921e + 04)$	5.483	$(-2.395,\ 13.36)$
$i = 3$	—	—	-473.4	$(-1249,\ 302.2)$

TABLE 21: R_{-1} vs. Entropy.

	p_i	CI	q_i	CI
$i = 1$	$-7.6e + 05$	$(-4.028e + 08,\ 4.013e + 08)$	135.2	$(-7.287e + 04,\ 7.314e + 04)$
$i = 2$	$-2.077e + 06$	$(-1.1e + 09,\ 1.096e + 09)$	$-1.259e + 04$	$(-6.675e + 06,\ 6.65e + 06)$
$i = 3$	$-1.406e + 06$	$(-7.444e + 08,\ 7.415e + 08)$	$-2.283e + 04$	$(-1.208e + 07,\ 1.204e + 07)$

Table 22: $R_{1/2}$ vs. Entropy.

	p_i	CI	q_i	CI
$i=1$	$-1.575e+06$	$(-1.165e+09,\ 1.162e+09)$	102.9	$(-7.795e+04,\ 7.816e+04)$
$i=2$	$-4.215e+06$	$(-3.115e+09,\ 3.106e+09)$	$-2.721e+04$	$(-2.013e+07,\ 2.008e+07)$
$i=3$	$-2.775e+06$	$(-2.049e+09,\ 2.044e+09)$	$-4.406e+04$	$(-3.254e+07,\ 3.245e+07)$

Table 23: $R_{-1/2}$ vs. Entropy.

	p_i	CI	q_i	CI
$i=1$	$2.454e+04$	$(-2.946e+04,\ 7.854e+04)$	-6.267	$(-14.22,\ 1.686)$
$i=2$	$6.443e+04$	$(-8.139e+04,\ 2.102e+05)$	416.8	$(-493.2,\ 1327)$
$i=3$	$4.205e+04$	$(-5.534e+04,\ 1.394e+05)$	677.3	$(-891.1,\ 2246)$

Table 24: ABC vs. Entropy.

	p_i	CI	q_i	CI
$i=1$	$8.579e+05$	$(-2.287e+10,\ 2.287e+10)$	308	$(-8.305e+06,\ 8.306e+06)$
$i=2$	$2.692e+06$	$(-7.184e+10,\ 7.185e+10)$	$1.379e+04$	$(-3.674e+08,\ 3.675e+08)$
$i=3$	$1.993e+06$	$(-5.323e+10,\ 5.323e+10)$	$3.185e+04$	$(-8.508e+08,\ 8.508e+08)$

Table 25: GA vs. Entropy.

	p_i	CI	q_i	CI
$i=1$	-5810	$(-1.493e+04,\ 3315)$	-3.43	$(-5.625,\ -1.235)$
$i=2$	-6784	$(-1.739e+04,\ 3818)$	5.695	$(-2.055,\ 13.45)$
$i=3$	—	—	-108	$(-277.2,\ 61.22)$

Table 26: M_1 vs. Entropy.

	p_i	CI	q_i	CI
$i=1$	9765	$(-4.435e+04,\ 6.388e+04)$	-3.054	$(-8.9,\ 2.792)$
$i=2$	$1.127e+04$	$(-5.105e+04,\ 7.358e+04)$	3.672	$(-15.14,\ 22.48)$
$i=3$	—	—	-4.83	$(-34.52,\ 24.86)$
$i=4$	—	—	177.9	$(-806.6,\ 1162)$

Table 27: M_2 vs. Entropy.

	p_i	CI	q_i	CI
$i=1$	$2.117e+04$	$(421.2,\ 4.192e+04)$	-3.726	$(-5.577,\ -1.875)$
$i=2$	$2.408e+04$	$(522.6,\ 4.765e+04)$	378.5	$(8.47,\ 748.6)$

Table 28: $\overline{M}_1$ vs. Entropy.

	p_i	CI	q_i	CI
$i=1$	$-6.943e+06$	$(-2.572e+11,\ 2.572e+11)$	4530	$(-1.679e+08,\ 1.679e+08)$
$i=2$	$-5.788e+06$	$(-2.144e+11,\ 2.144e+11)$	$-3.523e+04$	$(-1.305e+09,\ 1.305e+09)$
$i=3$	—	—	$-7.099e+04$	$(-2.63e+09,\ 2.63e+09)$

Table 29: $\overline{M}_2$ vs. Entropy.

	p_i	CI	q_i	CI
$i = 1$	$4.171e+06$	$(-3.796e+11, 3.796e+11)$	3482	$(-3.171e+08, 3.171e+08)$
$i = 2$	$3.268e+06$	$(-2.975e+11, 2.975e+11)$	$-1.149e+04$	$(-1.045e+09, 1.045e+09)$
$i = 3$	—	—	$2.548e+04$	$(-2.319e+09, 2.319e+09)$
$i = 4$	—	—	$4.081e+04$	$(-3.714e+09, 3.715e+09)$

Table 30: AZI vs. Entropy.

	p_i	CI	q_i	CI
$i = 1$	$5.214e+06$	$(-1.034e+09, 1.044e+09)$	166.1	$(-3.334e+04, 3.367e+04)$
$i = 2$	$5.886e+06$	$(-1.167e+09, 1.179e+09)$	$9.2e+04$	$(-1.825e+07, 1.843e+07)$

Table 31: F vs. Entropy.

	p_i	CI	q_i	CI
$i = 1$	$3.363e+04$	$(-1.563e+05, 2.236e+05)$	-3.023	$(-8.886, 2.84)$
$i = 2$	$3.825e+04$	$(-1.777e+05, 2.542e+05)$	3.538	$(-15.15, 22.22)$
$i = 3$	—	—	-4.576	$(-33.6, 24.45)$
$i = 4$	—	—	600.1	$(-2788, 3988)$

Table 32: $ReZG_1$ vs. Entropy.

	p_i	CI	q_i	CI
$i = 1$	$2.858e+04$	$(-3.576e+04, 9.292e+04)$	-6.187	$(-14.22, 1.843)$
$i = 2$	$7.425e+04$	$(-9.781e+04, 2.463e+05)$	490.1	$(-606, 1586)$
$i = 3$	$4.793e+04$	$(-6.582e+04, 1.617e+05)$	768.1	$(-1054, 2590)$

Table 33: $ReZG_2$ vs. Entropy.

	p_i	CI	q_i	CI
$i = 1$	$5.915e+04$	$(-7.923e+04, 1.975e+05)$	-5.968	$(-14.01, 2.073)$
$i = 2$	$1.495e+05$	$(-2.114e+05, 5.104e+05)$	1035	$(-1380, 3450)$
$i = 3$	$9.381e+04$	$(-1.386e+05, 3.262e+05)$	1483	$(-2190, 5155)$

Table 34: $ReZG_3$ vs. Entropy.

	p_i	CI	q_i	CI
$i = 1$	$8.157e+04$	$(3.2e+04, 1.311e+05)$	1448	$(566.3, 2329)$
$i = 2$	$2.083e+05$	$(7.129e+04, 3.454e+05)$	2048	$(618.7, 3478)$
$i = 3$	$1.311e+05$	$(3.961e+04, 2.227e+05)$	—	—

where $x = F$ is rescaled through $\varepsilon = 8728$ and $\gamma = 7669$.

(xiii) Estimated rational polynomial of Entropy vs. $ReZG_1$ is

$$\text{Entropy}(x) = \frac{p_1x^2 + p_2x + p_3}{x^3 + q_1x^2 + q_2x + q_3}, \tag{56}$$

where $x = ReZG_1$ is rescaled through $\varepsilon = 222$ and $\gamma = 180.3$.

(xiv) Estimated rational polynomial of Entropy vs. $ReZG_2$ is

$$\text{Entropy}(x) = \frac{p_1x^2 + p_2x + p_3}{x^3 + q_1x^2 + q_2x + q_3}, \tag{57}$$

where $x = ReZG_2$ is rescaled through $\varepsilon = 618.6$ and $\gamma = 531.8$.

(xv) Estimated rational polynomial of Entropy vs. $ReZG_3$ is

TABLE 35: Goodness of fit for indices vs. entropy for $Nb0$.

Index	Fit type	SSE	R^2	Adjusted R^2	RMSE
R_1	rat13	0.002287	1	1	0.03382
R_{-1}	rat23	0.001106	1	1	0.03325
$R_{1/2}$	rat23	0.0006468	1	1	0.02543
$R_{-1/2}$	rat23	2.69e−05	1	1	0.005187
ABC	rat23	0.7225	1	0.9998	0.85
GA	rat13	0.0376	1	1	0.1371
M_1	rat14	0.002174	1	1	0.04663
M_2	rat12	0.01024	1	1	0.05843
$\overline{M}_1$	rat13	50.83	0.9973	0.992	5.041
$\overline{M}_2$	rat14	6.75	0.9996	0.9979	2.598
HM	rat23	9.678e−07	1	1	0.0009838
AZI	rat12	0.007279	1	1	0.04926
F	rat14	0.0002058	1	1	0.01434
$ReZG_1$	rat23	2.314e−05	1	1	0.00481
$ReZG_2$	rat23	7.752e−06	1	1	0.002784
$ReZG_3$	rat22	1.334e−05	1	1	0.002582

$$\text{Entropy}(x) = \frac{p_1x^2 + p_2x + p_3}{x^2 + q_1x + q_2}, \tag{58}$$

where $x = ReZG_3$ is rescaled through $\varepsilon = 2.974e + 04$ and $\gamma = 2.661e + 04$.

3. Conclusion

After determining the topological degree-based indices, the thermodynamical parameters of niobium (II) oxide are derived. Fitting curves and building mathematical models are used to create a relationship between each index and each thermodynamical property. In MATLAB software, the rational fitting method is utilized as it gives the least mean squared error of all the built-in methods.

Data Availability

The data used to support the findings of this study are cited at relevant places within the text as references.

Conflicts of Interest

The authors declare that they have no conflicts of interest.

Authors' Contributions

This work was equally contributed by all authors.

References

[1] Y. S. Prabhakar and M. K. Gupta, "Chemical structure indices in in silico molecular design," *Scientia Pharmaceutica*, vol. 76, no. 2, pp. 101–132, 2008.

[2] W. L. Jorgensen, "The many roles of computation in drug discovery," *Science*, vol. 303, no. 5665, pp. 1813–1818, 2004.

[3] H. Kubinyi, "QSAR and 3D QSAR in drug design Part 2: applications and problems," *Drug Discovery Today*, vol. 2, no. 12, pp. 538–546, 1997.

[4] R. Perkins, H. Fang, W. Tong, and W. J. Welsh, "Quantitative structure-activity relationship methods: perspectives on drug discovery and toxicology," *Environmental Toxicology and Chemistry*, vol. 22, no. 8, p. 1666, 2003.

[5] X. Zhang, M. K. Siddiqui, S. Javed, L. Sherin, F. Kausar, and M. H. Muhammad, "Physical analysis of heat for formation and entropy of ceria oxide using topological indices," *Combinatorial Chemistry & High Throughput Screening*, vol. 25, no. 3, pp. 441–450, 2022.

[6] Q. N. Hu, Y. Z. Liang, and K. T. Yi-Zeng, "The matrix expression, topological index and atomic attribute of molecular topological structure," *Journal of Data Science*, vol. 1, no. 4, pp. 361–389, 2021.

[7] F. Yamashita and M. Hashida, "In silico approaches for predicting ADME properties of drugs," *Drug Metabolism and Pharmacokinetics*, vol. 19, no. 5, pp. 327–338, 2004.

[8] J. C. Dearden, "In silico prediction of drug toxicity," *Journal of Computer-Aided Molecular Design*, vol. 17, no. 2, pp. 119–127, 2003.

[9] S. Ekins and S. A. Wrighton, "Application of in silico approaches to predicting drug-drug interactions," *Journal of Pharmacological and Toxicological Methods*, vol. 45, no. 1, pp. 65–69, 2001.

[10] I. Muegge, "Selection criteria for drug-like compounds," *Medicinal Research Reviews*, vol. 23, no. 3, pp. 302–321, 2003.

[11] X. Zhang, H. M. Awais, M. Javaid, and M. K. Siddiqui, "Multiplicative Zagreb indices of molecular graphs," *Journal of Chemistry*, vol. 2019, Article ID 5294198, 19 pages, 2019.

[12] W. P. Walters and B. B. Goldman, "Feature selection in quantitative structure-activity relationships," *Current opinion in drug discovery & development*, vol. 8, no. 3, pp. 329–333, 2005.

[13] P. Yu, J. Wu, S. Liu, J. Xiong, C. Jagadish, and Z. M. Wang, "Design and fabrication of silicon nanowires towards efficient solar cells," *Nano Today*, vol. 11, no. 6, pp. 704–737, 2016.

[14] M. K. Siddiqui, S. Javed, L. Sherin et al., "On analysis of topological properties for terbium IV oxide via enthalpy and entropy measurements," *Journal of Chemistry*, vol. 202116 pages, Article ID 5351776, 2021.

[15] X. Zhang, X. Wu, S. Akhter, M. K. Jamil, J. B. Liu, and M. R. Farahani, "Edge-version atom-bond connectivity and geometric arithmetic indices of generalized bridge molecular graphs," *Symmetry*, vol. 10, no. 12, p. 751, 2018.

[16] S. A. Razek, M. A. Swillam, and N. K. Allam, "Vertically aligned crystalline silicon nanowires with controlled

diameters for energy conversion applications: experimental and theoretical insights," *Journal of Applied Physics*, vol. 115, no. 19, Article ID 194305, 2014.

[17] N. Dhindsa, J. Walia, and S. S. Saini, "A platform for colorful solar cells with enhanced absorption," *Nanotechnology*, vol. 27, no. 49, Article ID 495203, 2016.

[18] M. K. Siddiqui, M. Naeem, N. A. Rahman, and M. Imran, "Computing topological indices of certain networks," *Journal of Optoelectronics and Advanced Materials*, vol. 18, pp. 884–892, 2016.

[19] D. Adikaari and S. R. P. Silva, "Thickness dependence of properties of excimer laser crystallized nano-polycrystalline silicon," *Journal of Applied Physics*, vol. 97, no. 11, Article ID 114305, 2005.

[20] X. Zhang, H. Jiang, J. B. Liu, and Z. Shao, "The cartesian product and join graphs on edge-version atom-bond connectivity and geometric arithmetic indices," *Molecules*, vol. 23, no. 7, p. 1731, 2018.

[21] Z. Shao, M. K. Siddiqui, and M. H. Muhammad, "Computing zagreb indices and zagreb polynomials for symmetrical nanotubes," *Symmetry*, vol. 10, no. 7, p. 244, 2018.

[22] Y. F. Tang, S. R. P. Silva, B. O. Boskovic, J. M. Shannon, and M. J. Rose, "Electron field emission from excimer laser crystallized amorphous silicon," *Applied Physics Letters*, vol. 80, no. 22, pp. 4154–4156, 2002.

[23] S. Jin, S. Hong, M. Mativenga et al., "Low temperature polycrystalline silicon with single orientation on glass by blue laser annealing," *Thin Solid Films*, vol. 616, pp. 838–841, 2016.

[24] X. Zhang, A. Rauf, M. Ishtiaq, M. K. Siddiqui, and M. H. Muhammad, "On degree based topological properties of two carbon nanotubes," *Polycyclic Aromatic Compounds*, vol. 42, no. 3, pp. 866–884, 2020.

[25] C. Wu, C. H. Crouch, L. Zhao et al., "Near-unity below-band-gap absorption by microstructured silicon," *Applied Physics Letters*, vol. 78, no. 13, pp. 1850–1852, 2001.

[26] A. J. Pedraza, J. D. Fowlkes, and D. H. Lowndes, "Silicon microcolumn arrays grown by nanosecond pulsed-excimer laser irradiation," *Applied Physics Letters*, vol. 74, no. 16, pp. 2322–2324, 1999.

[27] M. R. Gilbert, K. Arakawa, Z. Bergstrom et al., "Perspectives on multiscale modelling and experiments to accelerate materials development for fusion," *Journal of Nuclear Materials*, vol. 554, Article ID 153113, 2021.

[28] W. Gao, J. F. Conley, and Y. Ono, "NbO as gate electrode for n-channel metal-oxide-semiconductor field-effect-transistors," *Applied Physics Letters*, vol. 84, no. 23, pp. 4666–4668, 2004.

[29] S. H. Shin, T. Halpern, and P. M. Raccah, "High-speed high-current field switching of NbO2," *Journal of Applied Physics*, vol. 48, no. 7, pp. 3150–3153, 1977.

[30] A. L. Bowman, T. C. Wallace, J. L. Yarnell, and R. G. Wenzel, "The crystal structure of niobium monoxide," *Acta Crystallographica*, vol. 21, no. 5, p. 843, 1966.

[31] C. Nico, T. Monteiro, and M. P. F. Graça, "Niobium oxides and niobates physical properties: review and prospects," *Progress in Materials Science*, vol. 80, pp. 1–37, 2016.

[32] J. K. Hulm, C. K. Jones, R. A. Hein, and J. W. Gibson, "Superconductivity in the TiO and NbO systems," *Journal of Low Temperature Physics*, vol. 7, no. 3, pp. 291–307, 1972.

[33] M. A. Rashid, S. Ahmad, M. K. Siddiqui, and M. K. Kaabar, "On computation and analysis of topological index-based invariants for complex coronoid systems," *Complexity*, vol. 2021, Article ID 4646501, 12 pages, 2021.

[34] D. Amić, D. Bešlo, B. Lučić, S. Nikolić, and N. Trinajstić, "The vertex-connectivity index revisited," *Journal of Chemical Information and Computer Sciences*, vol. 38, no. 5, pp. 819–822, 1998.

[35] B. Bollobás and P. Erdos, "Graphs of extremal weights," *Ars Combinatoria*, vol. 50, pp. 225–233, 1998.

[36] E. Estrada, L. Torres, L. Rodriguez, and I. Gutman, "An atom-bond connectivity index: modelling the enthalpy of formation of alkanes," *Indian Journal of Chemistry*, vol. 37A, pp. 849–855, 1998.

[37] W. Gao, W. F. Wang, M. K. Jamil, R. Farooq, and M. R. Farahani, "Generalized atom-bond connectivity analysis of several chemical molecular graphs," *Bulgarian Chemical Communications*, vol. 48, no. 3, pp. 543–549, 2016.

[38] D. Vukičević and B. Furtula, "Topological index based on the ratios of geometrical and arithmetical means of end-vertex degrees of edges," *Journal of Mathematical Chemistry*, vol. 46, no. 4, pp. 1369–1376, 2009.

[39] K. C. Das and I. Gutman, "Some properties of the second Zagreb index," *MATCH Commun. Math. Comput. Chem*, vol. 52, no. 1, pp. 13–21, 2004.

[40] I. Gutman and N. Trinajstić, "Graph theory and molecular orbitals. Total φ-electron energy of alternant hydrocarbons," *Chemical Physics Letters*, vol. 17, no. 4, pp. 535–538, 1972.

[41] I. Gutman, B. Furtula, Z. K. Vukicevic, and G. Popivoda, "On Zagreb indices and coindices," *MATCH Commun. Math. Comput. Chem*, vol. 74, no. 1, pp. 5–16, 2015.

[42] I. Gutman and K. C. Das, "The first Zagreb index 30 years after," *MATCH Commun. Math. Comput. Chem*, vol. 50, no. 1, pp. 83–92, 2004.

[43] B. Furtula and I. Gutman, "A forgotten topological index," *Journal of Mathematical Chemistry*, vol. 53, no. 4, pp. 1184–1190, 2015.

[44] D. Wang, Y. Huang, and B. Liu, "Bounds on augmented zagreb index," *MATCH Commun. Math. Comput. Chem.*vol. 68, pp. 209–216, 2011.

[45] A. T. Balaban, "Highly discriminating distance-based topological index," *Chemical Physics Letters*, vol. 89, no. 5, pp. 399–404, 1982.

[46] A. T. Balaban and L. V. Quintas, "The smallest graphs, trees, and 4-trees with degenerate topological index," *Journal of Mathematical Chemistry*, vol. 14, pp. 213–233, 1983.

[47] P. S. Ranjini, V. Lokesha, and A. Usha, "Relation between phenylene and hexagonal squeeze using harmonic index," *Int. J. Graph Theory*, vol. 1, no. 4, pp. 116–121, 2013.